Mathematical Modelling of Partially Absorbing Boundaries in Biological Systems

by

Sarafa Adewale Iyaniwura

B.Sc., University of Ilorin, 2012

M.Sc., AIMS-Stellenbosch University, 2014

A THESIS SUBMITTED IN PARTIAL FULFILLMENT
OF THE REQUIREMENTS FOR THE DEGREE OF

Master of Science

in

THE FACULTY OF GRADUATE AND POSTDOCTORAL STUDIES

(Mathematics)

The University of British Columbia

(Vancouver)

August 2016

© Sarafa Adewale Iyaniwura, 2016

Abstract

This project presents a mathematical framework for identifying partially permeable biological boundaries, and estimating the rate of absorption of diffusing objects at such a boundary based on limited experimental data. We used partial differential equations (PDEs) to derive probability distribution functions for finding a particle performing Brownian motion in a region. These distribution functions can be fit to data to infer the existence of a boundary. We also used the probability distribution functions together with maximum likelihood estimation to estimate the rate of absorption of objects at the boundaries, based on simulated data. Furthermore, we consider a switching boundary and provide a technique for approximating the boundary with a partially permeable boundary.

Preface

This thesis is original, unpublished, independent work by the author, S. A. Iyaniwura under the supervision of Professor Daniel Coombs.

Table of Contents

List of Figures

Acknowledgments

I would like to express my sincere gratitude to my supervisor Daniel Coombs for believing in me, and also for his valuable and constructive suggestions throughout the planning and development of this thesis. I wish to acknowledge with much appreciation his guidance and encouragement during my studies.

A special gratitude to Michael Ward and Leah Keshet for taking their time to go through this thesis, and also for their constructive comments and suggestions. I appreciate your kindness.

In addition, I would like to say thank you to all the students, staff, and faculty members of the Institute of Applied Mathematics and the department of mathematics for their support, and also for being a great source of motivation. Thank you Dan for giving me the opportunity to be part of this wonderful department, institute, and the University of British Columbia in general.

Finally, I would like to thank my family and friends for their unlimited support and encouragement. I am very grateful and appreciate your love. I wish to dedicate this project to my late parents and my siblings.

Chapter 1

Introduction

1.1 Biological boundaries

Biological boundaries are barriers that separate a medium into different regions in the sense that a substance crossing from one region of the medium to another may experience some differences in its environment, and as a result react differently. In cell biology, it is known that proteins such as receptors are constantly diffusing on the cell surface. However, it is sometimes observed in experiments that some receptors experience restricted motion which leads to the speculation that there is a barrier preventing the free diffusion of these molecules. These barriers can either be formed by some other molecules diffusing on the cell surface, or by molecules that are confined to some region of the cell surface. Identifying these boundaries in experimental data is important because it will give us a profound understanding of the motion of the molecules involved. However, this may be challenging due to the size and quantity of the molecules, and the type of motion they undergo. Despite the importance of identifying these boundaries, not much has been done in developing mathematical techniques for accomplishing this task.

In this project, we present a mathematical framework for identifying partially permeable biological boundaries, and estimating the rate of absorption of diffusing objects at such a boundary based on limited experimental data. This technique is based on deriving a probability distribution function for finding a diffusing particle in a region at some specified time, and fitting the distribution function to data in

order to infer the existence of a boundary. The derived distribution function is also used together with maximum likelihood estimation to estimate the rate of absorption on the boundary. In addition, we looked at switching boundaries and present a technique for approximating the boundaries with partially permeable boundaries.

1.2 Definition of terms

Below are brief definitions of some of the biological terms used in this thesis.

1.2.1 Single Particle Tracking (SPT)

Single Particle Tracking (SPT) is a technique used to study the motion of an object in a medium [12]. This technique involves labelling the particle of interest with fluorescent optical labels. The sample containing this particle is placed under the microscope where it is excited using a laser light. When the fluorophores are excited, several pictures of the sample are taken over a period of time, and each picture frame is analyzed to obtain the (x,y) coordinates of the particle of interest at a particular time. These coordinates are then put together in order to create the trajectory of motion of the particle [9]. The tracks from SPT can be analyzed to determine the type of motion, and also heterogeneity in the motion of the particle, which gives information about the particle's interaction with its surrounding. Figure 1.1 shows an example of a trajectory from single particle tracking experiment.

1.2.2 Macrophage

A macrophage is a type of white blood cell that uses a process called phagocytosis to engulf and digest cellular debris, cancer cells, pathogens, and any other foreign substance that does not have the kind of protein specific of healthy cells on its surface [16]. Macrophages also help in regulating immune responses and participate in the development of inflammation by producing chemical substances such as enzymes, complement proteins, and interleukin-1, among others [16].

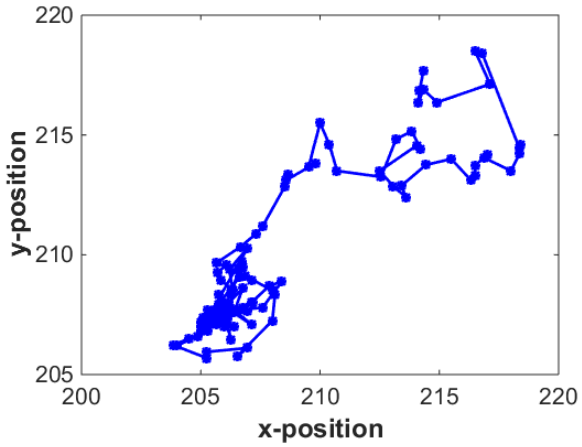

Figure 1.1: An example of a trajectory from single particle tracking experiment.

1.2.3 CD45

CD45 is a transmembrane protein tyrosine phosphatase that is abundantly expressed on the surface of various types of blood cells, including macrophages [11]. It plays an important role in the functioning of these cells, and can act as both positive and negative regulator of cellular signals [13].

1.2.4 Immunoglobulin G (IgG)

Immunoglobulin G is the most abundant type of antibody found in all body fluids [14]. It is produced and released by plasma B cells, and protects the body against bacterial, viral, and fungi infections by binding to the pathogens. An IgG molecule has a protein complex that is made up of four peptide-chains, comprising of two identical heavy chains and two identical light chains arranged in a Y-shape, and has two binding sites [14].

1.3 Motivation

This project is motivated by a Single Particle Tracking (SPT) experiment involving the tracking of the membrane phosphatase CD45 on macrophages. The experi-

mental set-up involves seeding macrophages that have CD45 molecules on their cell surface labelled with quantum dots on a coverslip. The coverslip is patterned with Immunoglobulin G (IgG), and the pattern consists of 2μm diameter circles with centres separated by 6μm, arranged in a regular 2D array as shown in Figure 1.2.

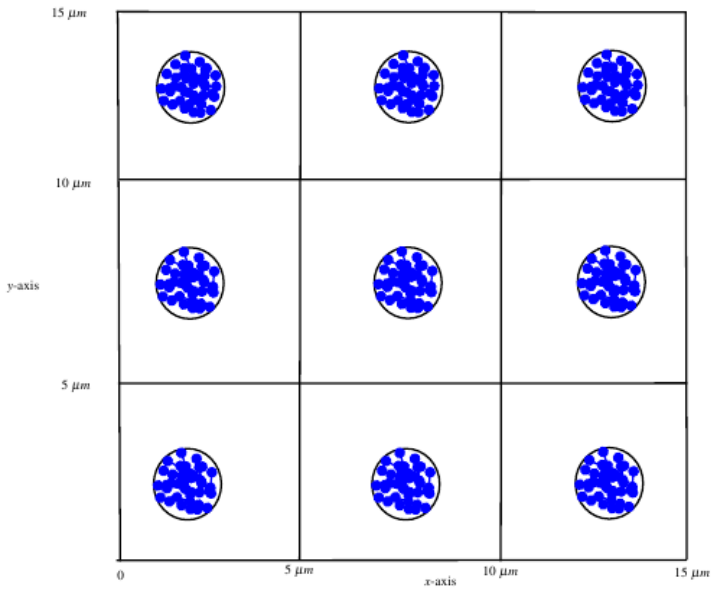

Figure 1.2: An illustration of the patterned coverslip. The circular regions are 2μm in diameter and contain the IgG (in blue). These regions are separated by a distance of 6μm from the centre of each region.

The macrophages are allowed to settle on the patterned coverslip, and when contact is formed between the macrophages and the IgG-patterned surface, the quantum dot-labelled CD45 molecules on the cell membrane are tracked for 10 seconds at a frequency of 30 Hz (hertz). During this experiment, it was observed that the contact of the macrophages with the immobile IgG creates a "zone of CD45 exclusion". While some of the phosphatase molecules that fall outside this zone appear to diffuse freely but bounce off the edge of the zone, those that fall inside the zone are observed to have restricted motion.

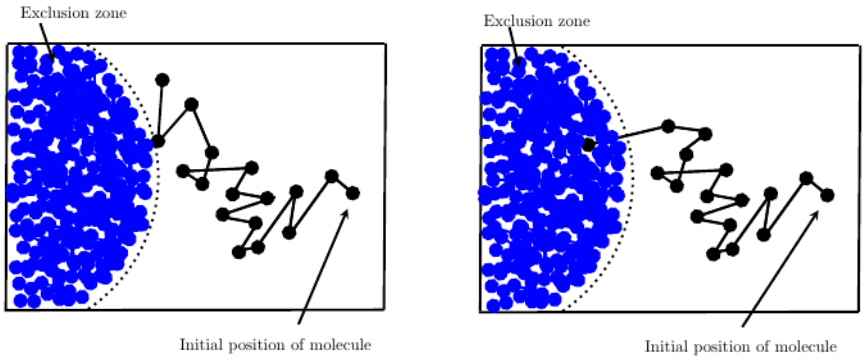

(a) A diffusing molecule bouncing off the exclusion zone.

(b) A diffusing molecule absorbed into the exclusion zone.

Figure 1.3: A sketch of one of the circular patterns on the coverslip and a diffusing molecule.

Figure 1.3a shows a trajectory bouncing off the boundary of an exclusion zone on the coverslip, while Figure 1.3b shows a trajectory that is absorbed into this zone. The apparent bouncing of phosphatase molecules from the zone of exclusion was observed from three different trajectories. However, there is not enough evidence to conclude whether the observations represent an anisotropic barrier exclusion effect on the trajectories, or the molecules are undergoing isotropic Brownian motion. In other words, the question is: *Are the trajectories actually bouncing off the "zone of CD45 exclusion"or we are observing simple Brownian motion?*

We approach this problem from the point of view of a particle performing Brownian motion in a domain, and derive the probability distribution function for finding the particle in some region after a specified time, considering different scenarios and geometries. Several previous works have studied the motion of a Brownian particle in a domain, and have derived probability distribution functions for the particle's position after some specified time [3], [5], [6], [7], and [10]. Chandrasekhar [3] derived the probability density function for finding a particle performing random walk at a point after taking some specified number of steps, from the point of view of a Bernoulli distribution. He considered the case of an unbounded domain, and a bounded domain with a reflecting boundary and an absorbing boundary. In this project, we derive probability distribution functions for a

particle performing Brownian motion in an unbounded domain, in a bounded domain with an absorbing boundary and a partially absorbing boundary using partial differential equations.

1.4 Brief description of chapters

Chapter two

In chapter two, we derive the diffusion equation as a continuous limit of a random walk, and then used the derived equation to set-up our mathematical problem. We also present a brief description of a partially absorbing boundary, Robin boundary condition, and maximum likelihood estimation.

Chapter three

In this chapter, we derive probability distribution functions for finding a particle performing Brownian motion in a region of an unbounded and a bounded domain. For the unbounded domain, we consider a semi-infinite rectangular region and a disk-shaped region, both with 'imaginary' boundaries, while for the bounded domain, we consider the right-half plane with an absorbing boundary at $x = 0$, and a disk-shaped region, also with an absorbing boundary. These probability distribution functions can be fit to data to infer the existence of a boundary.

Chapter four

In chapter four, we derive probability distribution functions for finding a particle performing Brownian motion in a domain that is bounded by a partially absorbing boundary. For this case, we also consider the right-half plane with a partially absorbing boundary at $x = 0$ and a disk-shaped region. We use these probability distribution functions together with maximum likelihood estimation to estimate the rate of absorption of particles on the partially absorbing boundaries. In addition, we calculate the mean and variance of first passage time for the particle performing Brownian motion to exit the regions.

Chapter five

In this chapter, we consider scenarios where the boundary of the domain in which the particle is performing Brownian motion switches from one boundary type to another over time. First, we consider the case where the boundary fluctuates between a perfectly reflecting boundary and different partially absorbing boundaries, and then use mean field approximation to replace the fluctuating boundary with a partially absorbing boundary. We also consider a case where the boundary switches between two specific boundary types, and provide a technique for approximating the switching boundary with a partially absorbing boundary.

Our goal in this project is to develop a mathematical technique for identifying partially permeable biological boundaries, and to estimate the rate of absorption on such boundaries. We also want to present a technique for approximating a switching boundary with a partially permeable boundary.

Chapter 2

Mathematical Problem Formulation

In this chapter, we derive the diffusion equation as a continuous limit of a random walk, and use the equation to formulate our mathematical problem. In addition, we present a brief introduction to a partially absorbing boundary, Robin boundary condition, and maximum likelihood estimation.

2.1 Random walk and the diffusion equation

A random walk is a path consisting of a succession of independent random steps. For example, the path traced by a molecule as it travels in a liquid or gas, the search path of a foraging animal, and the price of a fluctuating stock can all be modeled as random walks, although in reality, they may not be random (cf. [18]). Here, we shall show the relationship between a random walk and the diffusion equation.

Consider a particle performing random walk on a one dimensional lattice. Suppose the rule of its movement is that at each time step of size Δt, the particle can either jump to the left or right a distance of Δx with equal probability, $1/2$.

Let $P(x,t)$ be the probability that the particle is at position x at time t. Then according to the rule of movement of the particle, there are only two possibilities that the particle reaches position x at time $t+\Delta t$: The particle was at $x-\Delta x$ at time t and jumped to the right; or the particle was at $x+\Delta x$ at time t and jumped to the

left as shown in Figure 2.1.

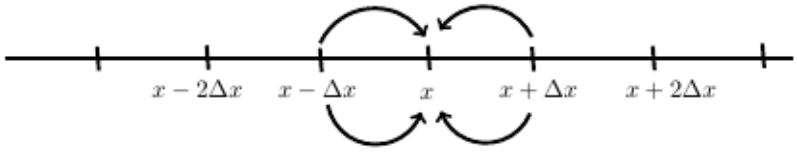

Figure 2.1: A random walk on one dimensional lattice. This figure shows the different possibilities of having a particle at position x at time $t+\Delta t$. The particle can either be at position $x-\Delta x$ at time t and take a step forward or at position $x+\Delta x$ at time t and take a step backward.

Since the next movement of the particle is independent of its present location, the probability that the particle is at position x at time $t+\Delta t$ given that it was at position $x-\Delta x$ at time t is $\frac{1}{2}P(x-\Delta x,t)$, while the probability that the particle is at position x at time $t+\Delta t$ given that it was at $x+\Delta x$ at time t is $\frac{1}{2}P(x+\Delta x,t)$. Thus, the probability that the particle is at position x at time $t+\Delta t$ is

$$P(x,t+\Delta t)=\frac{1}{2}P(x-\Delta x,t)+\frac{1}{2}P(x+\Delta x,t)\,. \tag{2.1}$$

Let us Taylor expand each term in this equation:

$$P(x,t+\Delta t)=P(x,t)+\frac{\partial}{\partial t}P(x,t)\Delta t+\mathscr{O}(\Delta t)^2\,, \tag{2.2}$$

$$P(x\pm\Delta x,t)=P(x,t)\pm\frac{\partial}{\partial x}P(x,t)\Delta x+\frac{1}{2}\frac{\partial^2}{\partial x^2}P(x,t)(\Delta x)^2+\mathscr{O}(\Delta x)^3\,. \tag{2.3}$$

Substituting the Taylor expansions into Equation (2.1) and simplifying, we have

$$\frac{\partial}{\partial t}P(x,t)\Delta t+\mathscr{O}(\Delta t)^2=\frac{1}{2}\frac{\partial^2}{\partial x^2}P(x,t)(\Delta x)^2+\mathscr{O}(\Delta x)^3\,.$$

Dividing through by Δt gives

$$\frac{\partial}{\partial t}P(x,t)+\mathscr{O}(\Delta t)=\frac{(\Delta x)^2}{2\Delta t}\frac{\partial^2}{\partial x^2}P(x,t)+\mathscr{O}\left(\frac{(\Delta x)^3}{\Delta t}\right)\,.$$

Next, we take the limit $\Delta x \longrightarrow 0$, $\Delta t \longrightarrow 0$ in such a way that $\lim \frac{(\Delta x)^2}{2\Delta t} = D$ exits, that is, D is finite: This special limit is called the diffusion limit. Thus, we have the diffusion equation

$$\frac{\partial}{\partial t}P(x,t) = D\frac{\partial^2}{\partial x^2}P(x,t)\,. \tag{2.4}$$

In n dimensions, similar calculations yield

$$\frac{\partial}{\partial t}P(\overrightarrow{x},t) = \nabla^2 P(\overrightarrow{x},t)\,, \tag{2.5}$$

where $\overrightarrow{x} \equiv (x_1,\ldots,x_n)$ is an n dimensional vector, D is the diffusion coefficient, and $\nabla^2 \equiv \left(\frac{\partial^2}{\partial x_1^2} + \cdots + \frac{\partial^2}{\partial x_n^2}\right)$ is the Laplace operator.

This shows that the diffusion equation is a continuous limit of a random walk process. Throughout this project, we shall use the diffusion equation in Equation (2.5) to model Brownian motion.

2.2 Mathematical formulation

Consider a particle performing Brownian motion in a two dimensional domain Ω. Let $P(\overrightarrow{\mathbf{x}},t|\overrightarrow{\mathbf{x}}_0,t_0)$ be the probability that the particle is at position $\overrightarrow{\mathbf{x}}$ at time t given that it started at point $\overrightarrow{\mathbf{x}}_0$ at time t_0. Then P satisfies

$$\begin{aligned} &\frac{\partial P}{\partial t} = D\nabla^2 P\,,\ \overrightarrow{\mathbf{x}} \in \Omega,\ t > t_0\,, \\ &P(\overrightarrow{\mathbf{x}},t_0|\overrightarrow{\mathbf{x}}_0,t_0) = \delta(\overrightarrow{\mathbf{x}} - \overrightarrow{\mathbf{x}}_0)\,, \qquad \overrightarrow{\mathbf{x}} \equiv (x,y)\,. \end{aligned} \tag{2.6}$$

If we let $\Gamma(t|\overrightarrow{\mathbf{x}}_0,t_0)$ be the probability that the particle is in a region R at time t given that it started at point $\overrightarrow{\mathbf{x}}_0 \in \Omega$ at time t_0, then

$$\Gamma(t|\overrightarrow{\mathbf{x}}_0,t_0) = \int_{\mathrm{R}} P(\overrightarrow{\mathbf{x}},t|\overrightarrow{\mathbf{x}}_0,t_0)\,\mathrm{d}A\,. \tag{2.7}$$

We shall solve the problem in Equation (2.6) in different geometries and with different types of boundary conditions.

2.3 Partially absorbing boundary and Robin boundary condition

A boundary is said to be partially absorbing if when a particle hits it, the particle is either reflected back into the domain or is absorbed by the boundary. Erban and Chapman [4] showed that a partially absorbing boundary can be accurately modelled using the Robin boundary condition;

$$D\frac{\partial}{\partial n}P(\overrightarrow{x},t) = \kappa P(\overrightarrow{x},t)\,, \tag{2.8}$$

where κ is the rate of absorption on the boundary, D is the diffusion coefficient of the particle, and $\frac{\partial}{\partial n}$ is the outward normal derivative on the boundary.

Note that when $\kappa = 0$ in Equation (2.8), the boundary condition corresponds to the perfectly reflecting boundary condition, $\frac{\partial}{\partial n}P(\overrightarrow{x},t) = 0$, while as κ tends to infinity, it becomes the perfectly absorbing boundary condition, that is, $P(\overrightarrow{x},t) = 0$. This shows that the Robin boundary condition is a weighted average of the reflecting and absorbing boundary conditions.

In the context of particle-based simulation, Erban and Chapman [4] went further to develop a relation between the probability of absorption upon hitting the boundary for a particle performing Brownian motion in a bounded domain and the rate of absorption in the Robin boundary condition (2.8). Their relation is given as

$$\kappa = 2\mathbb{P}\sqrt{\frac{D}{\pi\,\Delta t}}\,, \tag{2.9}$$

where $\mathbb{P}$ is the probability of absorption on the boundary, κ is the rate of absorption in the Robin boundary condition, and Δt is the time step used in the simulation.

Steven Andrews [1] also presented empirical relations between the Robin absorption rate and the probability of absorption on the boundary, and the relations are

$$\kappa' = \frac{1}{\sqrt{2\pi}}\mathbb{P} + 0.24761\,\mathbb{P}^2 + 0.00616\,\mathbb{P}^3 + 0.20384\,\mathbb{P}^4\,, \tag{2.10}$$

$$\mathbb{P} = \kappa'\sqrt{2\pi} - 3.33321\,\kappa'^2 + 3.35669\,\kappa'^3 - 1.52092\,\kappa'^4\,, \tag{2.11}$$

where $\kappa' = \kappa\sqrt{\frac{\Delta t}{2D}}$.

Unlike the relation presented by Erban and Chapman (in Equation (2.9)) which was derived analytically, Andrews relations were derived by fitting polynomials to simulated data [1].

2.4 Maximum Likelihood Estimation

A likelihood function is defined as a function of the parameters of a model given some observations or data [15]. Let $\mathbf{P}(\mathbf{X};\theta)$ be the probability of having the set of observations $\mathbf{X}$ given a set of parameters θ, then the likelihood function $\mathscr{L}(\theta|\mathbf{X})$, of having the parameter values θ given the outcomes $\mathbf{X}$ is given as [15]

$$\mathscr{L}(\theta|\mathbf{X}) \sim \mathbf{P}(\mathbf{X};\theta)\,.$$

Maximum Likelihood Estimation (MLE) is a method of estimating the parameters of a model based on some observations or data. In order words, for a fixed data and a corresponding model, MLE selects the set of values of the model parameters that maximizes the likelihood function.

Chapter 3

Identifying Biological Boundaries

In this chapter, we consider a particle performing Brownian motion in an unbounded domain and derive the probability distribution function for finding the particle at a position after a specified time. Then, we assume that there is a region of the unbounded domain that is bounded by an 'imaginary' boundary, and derive the probability distribution function for finding the particle in this region. The boundary is called imaginary because the diffusing particle is assumed to cross it from both directions without any restriction. In other words, the boundary does not have any effect on the motion of the particle. For the region bounded by the imaginary boundary, we consider a semi-infinite rectangular region and a disk-shaped region. In addition, we derive probability distribution functions for a particle performing Brownian motion in domains that are bounded by perfectly absorbing boundaries.

3.1 Unbounded domain: Imaginary boundary

Consider a particle performing Brownian motion in an unbounded two-dimensional domain as show in Figure 3.4. If we let Ω be the Cartesian plane, the probability that the particle is at position $\overrightarrow{\mathbf{x}}$ at time t given that it started at position $\overrightarrow{\mathbf{x}}_0$ at time $t = 0$, $P(\overrightarrow{\mathbf{x}}, t|\overrightarrow{\mathbf{x}}_0, 0)$ satisfies

$$\begin{aligned} &\frac{\partial P}{\partial t} = D\nabla^2 P, \ -\infty < x,y < \infty, \quad t > 0, \\ &\quad P(\overrightarrow{\mathbf{x}}, 0) = \delta(\overrightarrow{\mathbf{x}} - \overrightarrow{\mathbf{x}}_0). \end{aligned} \tag{3.1}$$

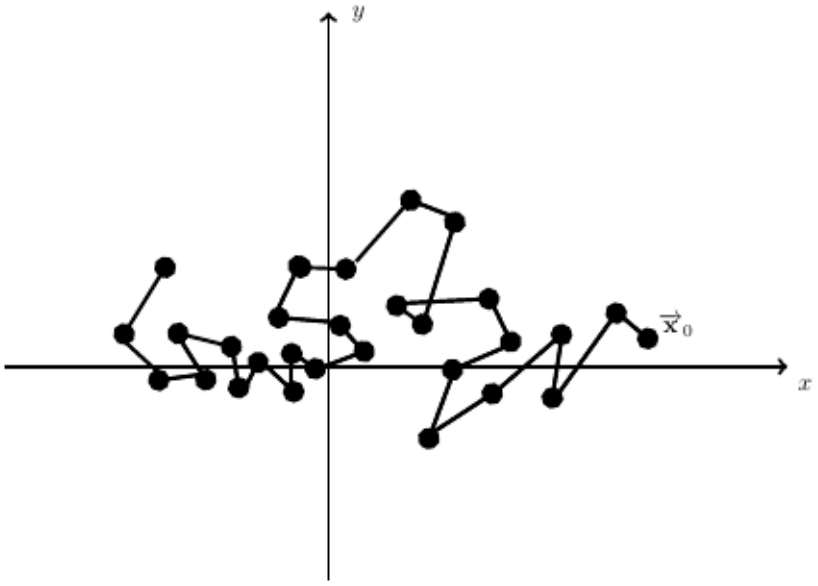

Figure 3.1: A particle performing Brownian motion in an unbounded two-dimensional domain.

We define the Fourier Transform (F.T.) of $P(x,y,t)$ as

$$\Im(k_1,k_2,t) = \frac{1}{(2\pi)^2}\int_{-\infty}^{\infty}\int_{-\infty}^{\infty} P(x,y,t)\, e^{-i(k_1x+k_2y)}\,\mathrm{d}x\,\mathrm{d}y\,, \tag{3.2}$$

and the inverse F.T. as

$$P(x,y,t) = \int_{-\infty}^{\infty}\int_{-\infty}^{\infty} \Im(k_1,k_2,t)\, e^{i(k_1x+k_2y)}\,\mathrm{d}k_1\,\mathrm{d}k_2\,. \tag{3.3}$$

Taking the F.T. of the PDE in Equation (3.1), we have

$$\frac{\mathrm{d}}{\mathrm{d}t}\Im(k_1,k_2,t) = -D(k_1^2+k_2^2)\,\Im(k_1,k_2,t)\,.$$

Solving this Ordinary Differential Equation (ODE) gives

$$\Im(k_1,k_2,t) = A\, e^{-D(k_1^2+k_2^2)t}\,, \tag{3.4}$$

where A is a constant.
Taking the F.T. of the initial condition in Equation (3.1), we have

$$\Im(k_1,k_2,0) = \frac{1}{(2\pi)^2}\, e^{-i(k_1x_0+k_2y_0)}\,. \tag{3.5}$$

Applying this initial condition to the solution in Equation (3.4) gives,

$$\Im(k_1,k_2,t) = \frac{1}{(2\pi)^2}\, e^{-D(k_1^2+k_2^2)t-i(k_1x_0+k_2y_0)}\,. \tag{3.6}$$

Let us take the inverse F.T. of Equation (3.6) using Equation (3.3).

$$P(x,y,t) = \int_{-\infty}^{\infty}\int_{-\infty}^{\infty} \frac{1}{(2\pi)^2}\, e^{-D(k_1^2+k_2^2)t-i(k_1x_0+k_2y_0)}\, e^{i(k_1x+k_2y)}\, \mathrm{d}k_1\, \mathrm{d}k_2\,.$$

Evaluating the integrals and simplifying gives

$$P(x,y,t|x_0,y_0,0) = \frac{1}{4\pi Dt}\, \exp\left(-\frac{1}{4Dt}[(x-x_0)^2 + (y-y_0)^2]\right). \tag{3.7}$$

This is the probability distribution function for finding a particle performing Brownian motion in an unbounded two-dimensional domain at position (x,y) at time t given that it started at position (x_0,y_0) at time $t=0$. It is important to point out that this equation is the free space Green's function for the diffusion equation in two-dimensions.

Suppose that there is an imaginary boundary at $x=a$ such that the Cartesian plane is divided into two regions as shown in Figure 3.2. We are interested in deriving the probability distribution functions for finding the particle in these regions at time t. Specifically, if we let $\Omega_1 = \{(x,y)|a \le x < \infty, -\infty < y < \infty\}$, we want to find the probability distribution function for finding the particle in Ω_1 at time t given that the particle started the Brownian motion at $(x_0,y_0) \in \Omega_1$ at time $t=0$. To get this distribution function, we need to integrate Equation (3.7) over Ω_1. That is,

$$\Gamma(t|x_0) = \int_{\Omega_1} P(x,y,t|x_0,y_0,0)\, \mathrm{d}A = \int_{-\infty}^{\infty}\int_{a}^{\infty} P(x,y,t|x_0,y_0,0)\, \mathrm{d}x\,\mathrm{d}y\,.$$

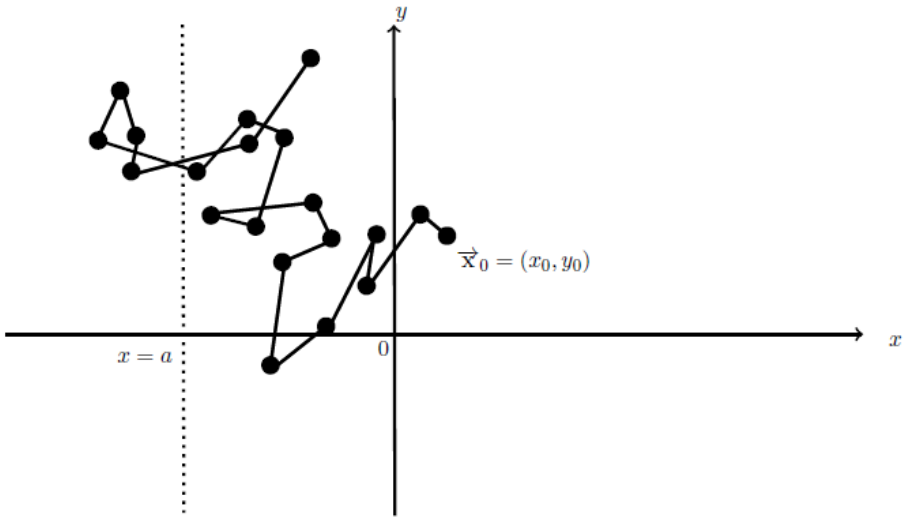

Figure 3.2: A particle performing Brownian motion in the Cartesian plane with an imaginary boundary at $\{(x,y)|x = a, -\infty < y < \infty\}$.

Substituting $P(x,y,t)$ as given in Equation (3.7) into this equation, we have

$$\Gamma(t|x_0) = \frac{1}{4\pi Dt} \int_{-\infty}^{\infty}\int_{a}^{\infty} \exp\left(-\frac{1}{4Dt}[(x-x_0)^2 + (y-y_0)^2]\right) \mathrm{d}x\,\mathrm{d}y.$$

Evaluating the integrals gives the probability distribution for finding the particle in Ω_1 over time,

$$\Gamma(t|x_0) = \frac{1}{2}\,\mathrm{erfc}\left(\frac{a-x_0}{\sqrt{4Dt}}\right), \tag{3.8}$$

where erfc(x)=1 - erf(x) is the complementary error function.

Figure 3.3 shows the plots of the probability distribution function in Equation (3.8). We observe from this figure that for each value of a, the probability of finding the particle in Ω_1 starts from one and decreases as time goes on. This is because the particle started the Brownian motion in Ω_1 and as time goes on, the chances of it crossing the imaginary boundary increases which leads to an increase in the probability of finding the particle in $\Omega \setminus \Omega_1$ as seen in Figure 3.3b. We also notice from the plots in this figure that the probability of finding the particle in each region after a specific time depends on the position of the imaginary boundary.

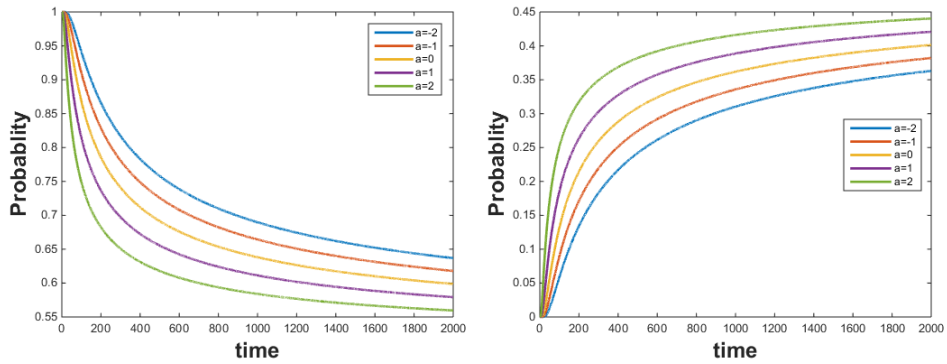

(a) Probability of finding the particle in Ω_1.

(b) Probability of finding the particle in $\Omega \setminus \Omega_1$.

Figure 3.3: The probability of finding a diffusing particle in one of the two half-planes of the Cartesian plane at time t, given that it started a Brownian motion at the point $x_0 = 5$, with diffusion coefficient $D = 0.1$, and an imaginary boundary at $x = a$.

Since the particle can cross the boundary from both directions without restriction, the probability of finding the particle in either of the two regions separated by the boundary converges to 0.5 after a long time. This can be seen by taking the limit of the probability distribution function in Equation (3.8) as t tends to infinity as shown below,

$$\lim_{t \longrightarrow \infty} \Gamma(t|x_0) = \lim_{t \longrightarrow \infty} \frac{1}{2} \operatorname{erfc}\left(\frac{a - x_0}{\sqrt{4Dt}}\right) = \frac{1}{2}.$$

Now, suppose the imaginary boundary bounds a disk-shaped region as shown in Figure 3.4. Then we need to integrate Equation (3.7) over the disk-shaped region to get the probability distribution function for finding the particle in this region at time t.

Before integrating, let us write the function in polar coordinates. From Equation (3.7), we have

$$P(\overrightarrow{\mathbf{x}}, t|\overrightarrow{\mathbf{x}}_0, 0) = \frac{1}{4\pi Dt} \exp\left(-\frac{|\overrightarrow{\mathbf{x}} - \overrightarrow{\mathbf{x}}_0|^2}{4Dt}\right). \tag{3.9}$$

Let $|\overrightarrow{\mathbf{x}}_0| = r_0$, and $|\overrightarrow{\mathbf{x}}| = r$ as shown in Figure 3.5. Using the cosine rule, the

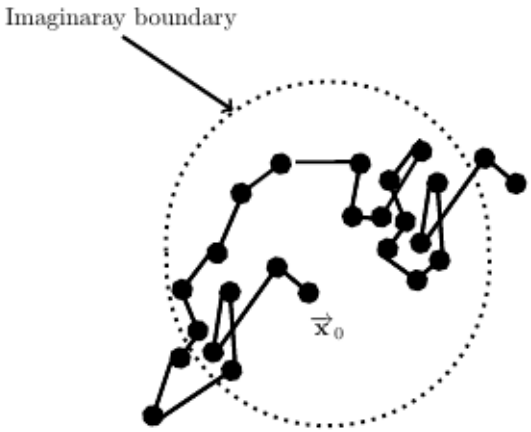

Figure 3.4: A particle performing Brownian motion in an unbounded domain, with an imaginary boundary bounding a disk-shaped region.

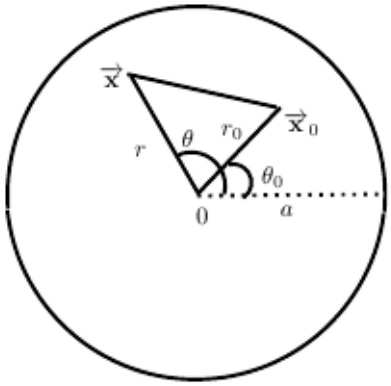

Figure 3.5: A sketch of the disk-shaped region.

probability distribution function in Equation (3.9) becomes

$$P(r,\theta,t) = \frac{1}{4\pi Dt}\exp\left(-\frac{1}{4Dt}(r^2+r_0^2-2rr_0\cos(\theta_0-\theta))\right). \tag{3.10}$$

Next, we integrate $P(r,\theta,t)$ over the disk-shaped region to get the probability dis-

tribution function for finding the particle in the region at time t. That is,

$$\Gamma(t|r_0) = \frac{1}{4\pi Dt}\int_0^{2\pi}\int_0^a \exp\left(-\frac{1}{4Dt}(r^2+r_0^2-2rr_0\cos(\theta_0-\theta))\right) r\,\mathrm{d}r\,\mathrm{d}\theta\,,$$

$$\Gamma(t|r_0) = \frac{1}{4\pi Dt}e^{\left(-\frac{r_0^2}{4Dt}\right)}\int_0^a re^{\left(-\frac{r^2}{4Dt}\right)}\left[\int_0^{2\pi}\exp\left(\frac{1}{4Dt}(2rr_0\cos(\theta_0-\theta))\right)\mathrm{d}\theta\right]\mathrm{d}r.$$

But

$$\int_0^{2\pi}\exp\left(\frac{1}{2Dt}(rr_0\cos(\theta_0-\theta))\right)\mathrm{d}\theta = 2\pi I_0\left(\frac{r_0 r}{2Dt}\right),$$

where $I_0(z)$ is the modified Bessel function of the first kind of order zero.

Therefore,

$$\Gamma(t|r_0) = \frac{1}{4\pi Dt}\exp\left(-\frac{r_0^2}{4Dt}\right)\left[2\pi\int_0^a r\exp\left(-\frac{r^2}{4Dt}\right) I_0\left(\frac{r_0 r}{2Dt}\right)\mathrm{d}r\right].$$

Evaluating the integral in this equation, we have

$$\Gamma(t|r_0) = \frac{1}{4\pi Dt}\exp\left(-\frac{r_0^2}{4Dt}\right)\left[4\pi Dt\exp\left(\frac{r_0^2}{4Dt}\right)\left(1-Q_1\left(\frac{r_0}{\sqrt{2Dt}},\frac{a}{\sqrt{2Dt}}\right)\right)\right].$$

Simplifying, we have the probability distribution function for finding the particle in the disk-shaped region at time t given that it start at a distance r_0 away from the center of the region,

$$\Gamma(t|r_0) = 1-Q_1\left(\frac{r_0}{\sqrt{2Dt}},\frac{a}{\sqrt{2Dt}}\right), \tag{3.11}$$

where Q_1 is the Marcum Q-function of order one.

The Marcum Q-function of order M Q_M is defined as

$$Q_M(a,b) = \int_b^\infty x\left(\frac{x}{a}\right)^{M-1}\exp\left(-\frac{x^2+a^2}{2}\right) I_{M-1}(ax)\,\mathrm{d}x, \tag{3.12}$$

where I_{M-1} is the modified Bessel function of the first kind of order $M-1$ [17].

Figure 3.6 shows the plots of the probability distribution function in Equation (3.11). In this figure, we fixed the initial position of the particle $r_0 = 5$, and varied

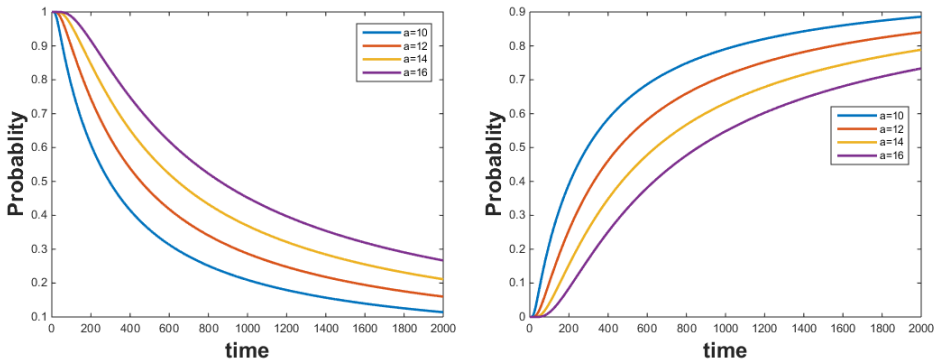

(a) Probability of finding the particle inside the disk-shaped region.

(b) Probability of finding the particle outside the disk-shaped region.

Figure 3.6: The probability of finding a particle performing Brownian motion inside a disk-shaped region of radius a with an imaginary boundary at time t, given that it started at a distance $r_0 = 5$ away from the center of the region and with diffusion coefficient $D = 0.1$.

the radius of the region. We notice from these plots that as the radius of the disk-shaped region increases, the probability that the particle is still in the region after a specific time increases. This shows that the probability of finding the particle in the region at some time $t > 0$ depends on the radius of the region. This is because the time required for the particle to reach the boundary increases as the region gets bigger. Similar to the plots of the distribution function in Equation (3.8), we observe that the probability of finding the particle inside the disk-shaped region starts from one and decreases with respect to time. The reason for this is that the particle started its motion inside the region and as time goes on, the chances of it crossing the imaginary boundary increases. In addition, the probability of finding the particle inside the disk-shaped region tends to zero after a long time. This can early be seen by taking the limit as t tends to infinity of the probability distribution function in Equation (3.11).

3.2 Bounded domain: Perfectly absorbing boundary

In this section, we derive probability distribution functions for a particle performing Brownian motion in a bounded domain with a perfectly absorbing boundary.

Since the boundary is perfectly absorbing, the diffusing particle vanishes immediately when it hits the boundary. We again consider two different geometries, the right half-plane (rectangular coordinates) and a disk-shaped region (polar coordinates).

3.2.1 The half-plane problem

Suppose we have a particle performing Brownian motion in the right half-plane with a perfectly absorbing boundary at $x = 0$ as shown in Figure 3.7. Let us define $\Omega = \{(x,y)\,|\,0 \leq x < \infty,\ -\infty < y < \infty\}$. We impose a Dirichlet (absorbing) boundary condition on the boundary at $x = 0$ for the problem in Equation (2.6) to get the problem for the probability of finding the particle at a point $\vec{\mathbf{x}}$ at time t given that it started at $\vec{\mathbf{x}}_0$ at time $t = 0$, $P(\vec{\mathbf{x}},t|\vec{\mathbf{x}}_0)$;

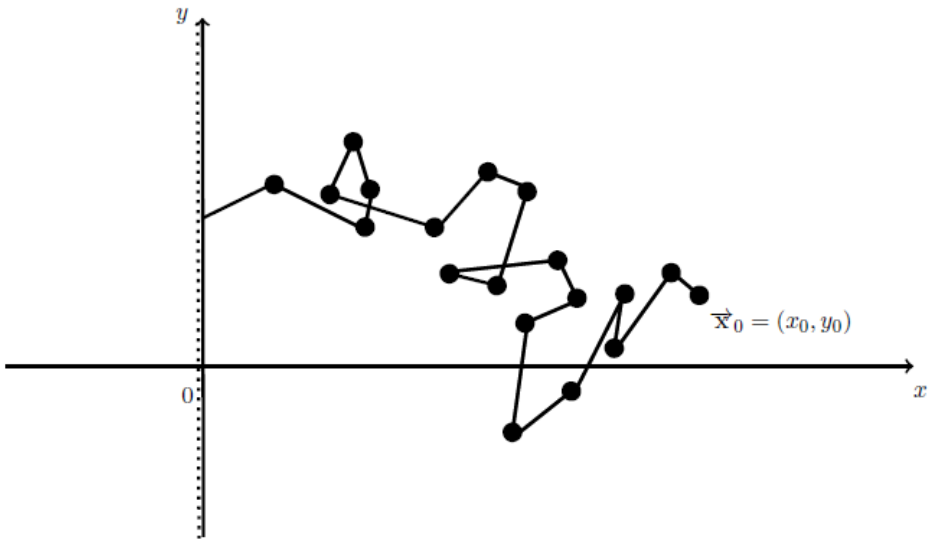

Figure 3.7: A particle performing Brownian motion in the right half-plane with an absorbing boundary at $x = 0$.

$$
\begin{aligned}
&\frac{\partial P}{\partial t} = D\nabla^2 P, \quad \vec{\mathbf{x}} \in \Omega, t > 0, \\
&P(\vec{\mathbf{x}}, 0) = \delta(\vec{\mathbf{x}} - \vec{\mathbf{x}}_0), \\
&P = 0, \ x = 0, -\infty < y < \infty, \\
&P \longrightarrow 0, \quad \text{as } x \longrightarrow \infty.
\end{aligned}
\tag{3.13}
$$

We shall rewrite this problem using the method of images which involves extending the domain Ω by adding its mirror image with respect to a symmetry hyperplane. Then we place a mirror image of the initial condition in the extended domain in such a way that the boundary condition $P = 0$ is satisfied at $x = 0$. The original

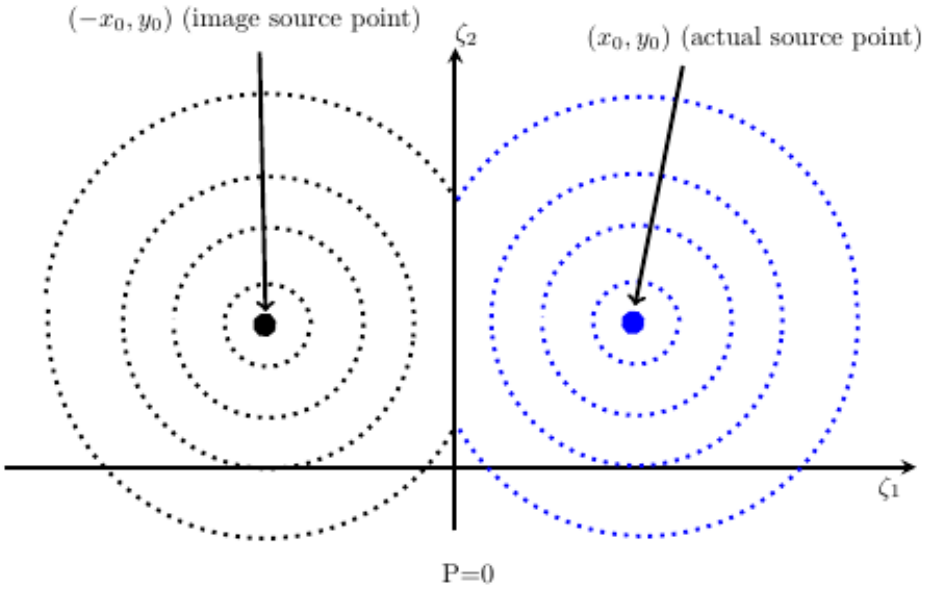

Figure 3.8: An illustration of the idea of method of images.

initial condition $\delta(x - x_0, y - y_0)$ is at (x_0, y_0), while the image initial condition $\delta(x + x_0, y - y_0)$ is placed at $(-x_0, y_0)$ as shown in Figure 3.8. So doing, the new

problem is

$$\begin{aligned}
&\frac{\partial P}{\partial t} = D\nabla^2 P, \quad -\infty < x,y < \infty,\ t > 0,\\
&P = 0,\ \text{on } x = 0,\ -\infty < y < \infty,\\
&P = \delta(x-x_0, y-y_0) - \delta(x+x_0, y-y_0),\ \text{at } t = 0\,.
\end{aligned} \tag{3.14}$$

We observe that our new initial condition is the difference of the actual and image initial conditions. This is required in order to satisfy the boundary condition $P = 0$ at $x = 0$.

Define the Fourier Transform (F.T.) of $P(x,y,t)$ as,

$$\widehat{P}(k_1,k_2,t) = \frac{1}{(2\pi)^2}\int_{-\infty}^{\infty}\int_{-\infty}^{\infty} P(x,y,t)\, e^{-i(k_1x+k_2y)}\,\mathrm{d}x\,\mathrm{d}y\,, \tag{3.15}$$

and the inverse F.T. as

$$P(x,y,t) = \int_{-\infty}^{\infty}\int_{-\infty}^{\infty} \widehat{P}(k_1,k_2,t)\, e^{i(k_1x+k_2y)}\,\mathrm{d}k_1\,\mathrm{d}k_2\,. \tag{3.16}$$

Taking the F.T. of the PDE in Equation (3.14),

$$\begin{aligned}
&\frac{1}{(2\pi)^2}\int_{-\infty}^{\infty}\int_{-\infty}^{\infty} P_t(x,y,t)\, e^{-i(k_1x+k_2y)}\,\mathrm{d}x\,\mathrm{d}y =\\
&\qquad D\frac{1}{(2\pi)^2}\int_{-\infty}^{\infty}\int_{-\infty}^{\infty} \nabla^2 P(x,y,t)\, e^{-i(k_1x+k_2y)}\,\mathrm{d}x\,\mathrm{d}y\,,\\
&\widehat{P}(k_1,k_2,t) = -D(k_1^2+k_2^2)\,\widehat{P}(k_1,k_2,t)\,.
\end{aligned}$$

Solving this equation, we have

$$\widehat{P}(k_1,k_2,t) = A\, e^{-D(k_1^2+k_2^2)t}\,, \tag{3.17}$$

where A is a constant.
Taking the F.T. of the initial condition in Equation (3.14), we have

$$\widehat{P}(k_1,k_2,0) = \frac{1}{(2\pi)^2}\left(e^{-i(k_1x_0+k_2y_0)} - e^{-i(k_1x_0-k_2y_0)}\right).$$

Applying this initial condition to the solution in Equation (3.17), we obtain

$$\widehat{P}(k_1,k_2,\sigma) = \frac{1}{(2\pi)^2}\left(e^{-i(k_1x_0+k_2y_0)} - e^{-i(k_1x_0-k_2y_0)}\right)e^{-D(k_1^2+k_2^2)t}\,.$$

Now, let us take the inverse F.T. of this equation using Equation (3.16),

$$\begin{aligned}P(x,y,t) = {} & \frac{1}{(2\pi)^2}\int_{-\infty}^{\infty}\int_{-\infty}^{\infty} e^{-D(k_1^2+k_2^2)t+i[k_1(x-x_0)+k_2(y-y_0)]}\,\mathrm{d}k_1\,\mathrm{d}k_2 \\ & + \frac{1}{(2\pi)^2}\int_{-\infty}^{\infty}\int_{-\infty}^{\infty} e^{-D(k_1^2+k_2^2)t+i[k_1(x+x_0)+k_2(y-y_0)]}\,\mathrm{d}k_1\,\mathrm{d}k_2\,.\end{aligned}$$

Evaluating these integrals using the fact that

$$\int_{-\infty}^{\infty} e^{-Dk_1^2t+ik(z-x)}\,\mathrm{d}k = \left(\frac{\pi}{Dt}\right)^{1/2}\exp\left(\frac{(z-x)^2}{4Dt}\right),$$

we obtain the probability distribution function for finding a particle performing Brownian motion in the right half-plane at position $\overrightarrow{\mathbf{x}}$ at time t given that it started from the point $\overrightarrow{\mathbf{x}}_0$ at $t=0$, and that there is an absorbing boundary at $x=0$,

$$\begin{aligned}P(\overrightarrow{\mathbf{x}},t|\overrightarrow{\mathbf{x}}_0) = \frac{1}{4D\pi t}\Bigg[& \exp\left(-\frac{[(x-x_0)^2+(y-y_0)^2]}{4Dt}\right) \\ & -\exp\left(-\frac{[(x+x_0)^2+(y-y_0)^2]}{4Dt}\right)\Bigg], \quad x>0\,.\end{aligned} \tag{3.18}$$

To get the probability distribution function for finding the particle in the right half-plane at time t, we need to integrate $P(\overrightarrow{\mathbf{x}},t|\overrightarrow{\mathbf{x}}_0)$ over the region. That is,

$$\Gamma(t|x_0) = \int_{-\infty}^{\infty}\int_{0}^{\infty} P(x,y,t|x_0,y_0)\,\mathrm{d}x\,\mathrm{d}y\,.$$

Substituting $P(x,y,t|x_0,y_0)$ as given in Equation (3.18) into this equation,

$$\begin{aligned}\Gamma(t|x_0) = \frac{1}{4D\pi t}\int_{-\infty}^{\infty}\int_{0}^{\infty} \Bigg[& \exp\left(-\frac{[(x-x_0)^2+(y-y_0)^2]}{4Dt}\right) \\ & -\exp\left(-\frac{[(x+x_0)^2+(y-y_0)^2]}{4Dt}\right)\Bigg]\,\mathrm{d}x\,\mathrm{d}y\,.\end{aligned}$$

Evaluating these integrals, we obtain

$$\Gamma(t|x_0) = \frac{1}{2}\left[\operatorname{erfc}\left(-\frac{x_0}{\sqrt{4Dt}}\right) - \operatorname{erfc}\left(\frac{x_0}{\sqrt{4Dt}}\right)\right]. \tag{3.19}$$

Thus, this is the probability distribution function for finding the particle in the right half-plane at time t, while $1-\Gamma(t|x_0)$ is the probability that the particle has been absorbed by the boundary at time t.

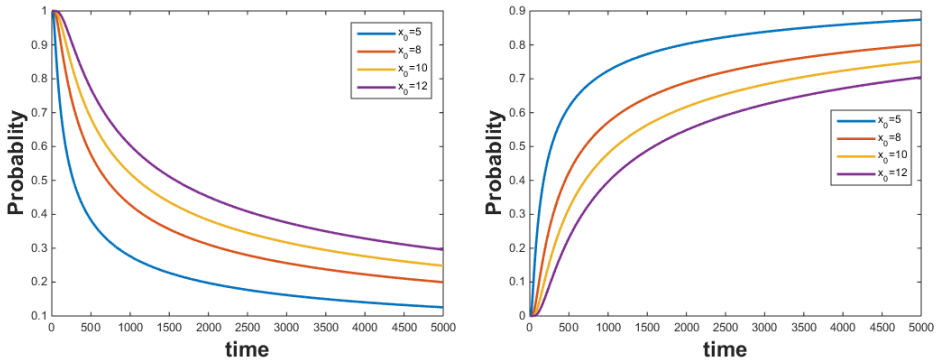

(a) Probability of finding the particle in the right half-plane at time t.

(b) Probability that the particle has been absorbed by the boundary at time t.

Figure 3.9: The probability of finding a particle performing a Brownian motion in the right-half plane at time t given that it started at the point x_0, with $D = 0.1$, and that there is a perfectly absorbing boundary at $x = 0$.

We notice from the plots of the probability distribution function in Equation (3.19) shown in Figure 3.9 that the probability that the diffusing particle is still in the right half-plane at time t depends on the initial position of the particle. As the particle starts farther away from the boundary, the time required for the particle to reach the boundary increases, therefore, the probability of finding the particle in the region also increases. We also observe from this figure that the probability of finding the particle in the right half-plane at the beginning ($t = 0$) is 1, and it decreases with respect to an increase in time. This is because the particle started its motion in the right half-plane and as time goes on, the chances of it getting absorbed by the boundary increases. After a long time, the probability that the particle is still in the right half-plane tends to zero. This is logical because we

would expect the particle to have been absorbed by the boundary after a long time since P tends to zero as x tends to infinity. This can easily be seen by taking the limit of the probability distribution function in Equation (3.19) as t tends to infinity.

3.2.2 The disk problem

Suppose the particle performing Brownian motion is in a disk-shaped domain of radius a, with a perfectly absorbing boundary at $r = a$ as shown in Figure 3.10. Let Ω

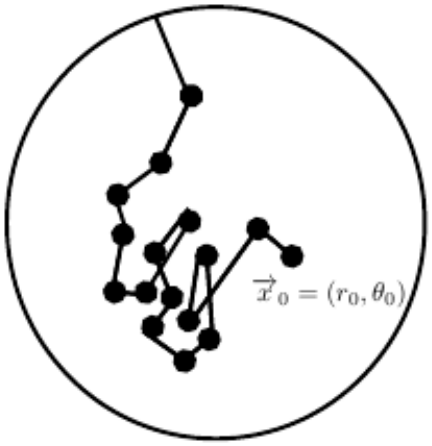

Figure 3.10: A particle performing Brownian motion in a disk-shaped region with a perfectly absorbing boundary.

be the interior of the disk-shaped region, that is, $\Omega = \{(r,\theta) \,|\, 0 < r \leq a, 0 \leq \theta \leq 2\pi\}$. Then the probability that the particle is at position $\vec{\mathbf{x}} \in \Omega$ at time t given that it started at point $\vec{\mathbf{x}}_0 \in \Omega$ at time $t = 0$ satisfies

$$\begin{aligned} &\frac{\partial P}{\partial t} = D\nabla^2 P, \ \vec{\mathbf{x}} = (r,\theta) \in \Omega, \, t > 0\,, \\ &P(\vec{\mathbf{x}}, 0) = \delta(\vec{\mathbf{x}} - \vec{\mathbf{x}}_0)\,, \\ &P = 0\,, \ \text{on } r = a, \, 0 \leq \theta \leq 2\pi\,. \end{aligned} \tag{3.20}$$

We shall solve this problem using Green's function and the method of images

for a disk. First, we rewrite the problem by writing the delta function in the initial condition as a forcing in the PDE, that is,

$$\begin{aligned} \frac{\partial P}{\partial t} =& D\nabla^2 P + \delta(\overrightarrow{\mathbf{x}} - \overrightarrow{\mathbf{x}}_0)\,\delta(t),\ \overrightarrow{\mathbf{x}} \in \Omega,\ t > 0, \\ & P = 0,\ \text{on } \partial\Omega, \\ & P \equiv 0,\ \text{at } t = 0. \end{aligned} \tag{3.21}$$

Let G_f be the free space Green's function for the diffusion equation which satisfies

$$\begin{aligned} \frac{\partial G_f}{\partial t} =& D\nabla^2 G_f + \delta(\overrightarrow{\mathbf{x}} - \overrightarrow{\mathbf{x}}_0)\,\delta(t),\ \overrightarrow{\mathbf{x}} \in \Omega,\ t > 0, \\ & G_f \equiv 0,\ \text{at } t = 0. \end{aligned}$$

Then from Equation (3.9), we have that the free space Green's function is

$$G_f = \frac{1}{4\pi D t} \exp\left(-\frac{|\overrightarrow{\mathbf{x}} - \overrightarrow{\mathbf{x}}_0|^2}{4Dt} \right). \tag{3.22}$$

The idea of the method of images is to find a harmonic function $\mathbb{H}$ which satisfies the PDE in Equation (3.20), such that $P = G_f + \mathbb{H}$, with $\mathbb{H} = -G_f$ on $\partial\Omega$.

Let $r = |\overrightarrow{\mathbf{x}}|$, $r_0 = |\overrightarrow{\mathbf{x_0}}|$, $r_1 = |\overrightarrow{\mathbf{x}} - \overrightarrow{\mathbf{x_0}}|$, $r_2 = |\overrightarrow{\mathbf{x_0}} - \overrightarrow{\zeta}|$ as shown in Figure 3.11. Then in polar coordinates, Equation (3.22) becomes

$$G_f = \frac{1}{4\pi D t} \exp\left(-\frac{r_1^2}{4Dt} \right). \tag{3.23}$$

We know that $r_2 = r_1 \left(\frac{a}{r}\right)$ whenever $r_0 = a$. Therefore, we choose the harmonic function $\mathbb{H}$ to be

$$\mathbb{H} = \frac{1}{4\pi D t} \exp\left(-\frac{C r_2^2}{4Dt} \right),$$

where C is a constant to be determined.

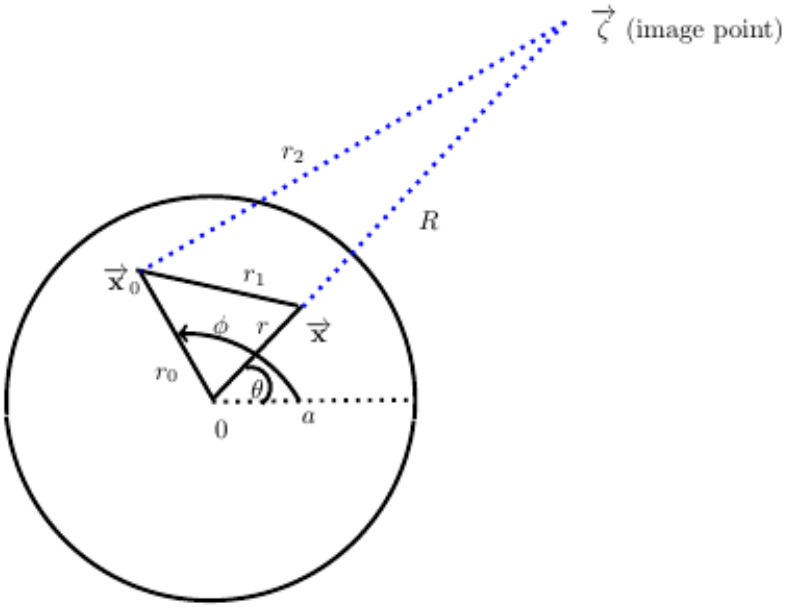

Figure 3.11: A sketch of the method of images for a disk.

Now set $P = G_f + \mathbb{H}$ and we achieve

$$P = \frac{1}{4\pi Dt}\left[\exp\left(-\frac{r_1^2}{4Dt}\right) - \exp\left(-\frac{Cr_2^2}{4Dt}\right)\right]. \tag{3.24}$$

Next, we need to find the constant C so that P satisfies the boundary condition. Using the fact that when $r_0 = a$, $r_2 = r_1\left(\frac{a}{r}\right)$ and the boundary condition $P = 0$, we obtained $C = \frac{r^2}{a^2}$, and so

$$P = \frac{1}{4\pi Dt}\left[\exp\left(-\frac{r_1^2}{4Dt}\right) - \exp\left(-\frac{r^2 r_2^2}{4a^2 Dt}\right)\right]. \tag{3.25}$$

But from Figure 3.11, using the cosine rule, we have

$$\begin{aligned} r_1^2 &= r^2 + r_0^2 - 2rr_0\cos(\theta_0 - \theta), \\ r_2^2 &= \frac{1}{r^2}(a^4 + r^2 r_0^2 - 2a^2 rr_0\cos(\theta_0 - \theta)). \end{aligned} \tag{3.26}$$

Therefore,

$$P(r,\theta,t) = \frac{1}{4\pi Dt}\left[\exp\left(-\frac{1}{4Dt}(r^2+r_0^2-2rr_0\cos(\theta_0-\theta))\right)\right. \\ \left.-\exp\left(-\frac{1}{4a^2Dt}(a^4+r^2r_0^2-2a^2rr_0\cos(\theta_0-\theta))\right)\right]. \tag{3.27}$$

This is the probability distribution function for finding a particle performing Brownian motion in a disk-shaped region of radius a, at a point (r,θ) inside the region, given that it started at a point (r_0,θ_0) and that there is a perfectly absorbing boundary at $r=a$. We need to integrate this function over the disk-shaped region to get the probability distribution function of finding the particle inside the region at time t. That is,

$$\Gamma(t|r_0) = \int_\Omega P(r,\theta,t)\,\mathrm{d}\overrightarrow{\mathbf{x}} = \int_0^{2\pi}\int_0^a P(r,\theta,t)\,r\,\mathrm{d}r\,\mathrm{d}\theta\,.$$

Substituting Equation (3.27) into this equation,

$$\Gamma(t|r_0) = \frac{1}{4\pi Dt}\left[\int_0^{2\pi}\int_0^a \exp\left(-\frac{1}{4Dt}(r^2+r_0^2-2rr_0\cos(\theta_0-\theta))\right)\,r\,\mathrm{d}r\,\mathrm{d}\theta\right. \\ \left.\int_0^{2\pi}\int_0^a \exp\left(-\frac{1}{4a^2Dt}(a^4+r^2r_0^2-2a^2rr_0\cos(\theta_0-\theta))\right)\,r\,\mathrm{d}r\,\mathrm{d}\theta\right].$$

Evaluating these integrals using the same approach we used in the case of a disk-shaped region with an imaginary boundary, we have

$$\Gamma(t|r_0) = \left(1-Q_1\left(\frac{r_0}{\sqrt{2Dt}},\frac{a}{\sqrt{2Dt}}\right)\right) \\ -\exp\left(\frac{r_0^2-a^2}{4Dt}\right)\left(1-Q_1\left(\frac{ar_0}{\sqrt{2aDt}},\frac{a}{\sqrt{2aDt}}\right)\right), \tag{3.28}$$

where Q_1 is the Marcum Q-function of order one defined in Equation (3.12).

Remark 3.2.3. *The disk problem for a partially absorbing boundary cannot be solved by the method of images because we cannot find the constant C (in Equation* (3.24)*) for which P satisfies the Robin boundary condition. Although, other methods such as separation of variables and the conformal mapping method can*

be used to solve the problem.

Equation (3.28) is the probability distribution function for finding a particle performing Brownian motion in a disk-shaped region of radius a, given that it started at a distance r_0 away from the center of the region and that the region has a perfectly absorbing boundary. We notice that the distribution function is independent of θ. This shows that the probability of finding the particle in the region is independent of the angle of rotation of the disk. Figure 3.12 shows the plots of the distribution function in Equation (3.28). In this figure, we used a fixed initial position for the particle and varied the radius of the region. As we would expect, the probability of finding the particle in the disk-shaped region at time $t = 0$ is one since the particle started from inside the region. This probability decreases over time because the chances of the particle getting absorbed on the boundary increases as time goes on.

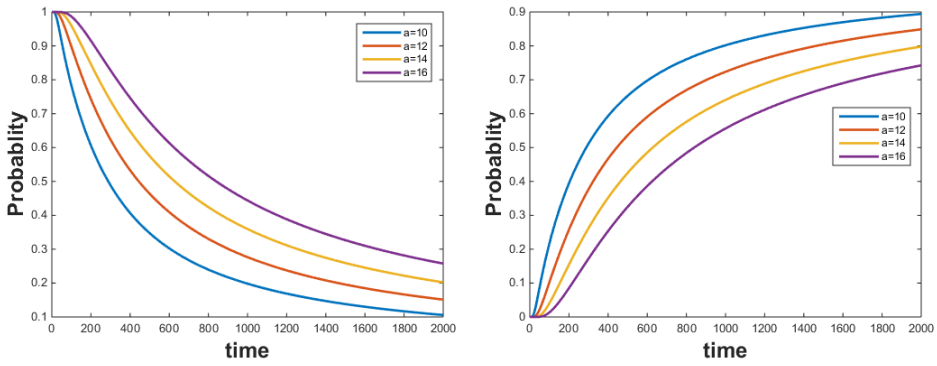

(a) Probability of finding the particle inside the disk-shaped region.

(b) Probability that the particle has been absorbed by the boundary at time t.

Figure 3.12: The probability of finding a particle performing Brownian motion inside a disk-shaped of radius a at time t, given that it started at a distance $r_0 = 5$ away form the center of the region, with $D = 0.1$, and that the region has a perfectly absorbing boundary.

We would also expect the probability of finding the particle inside the region to converge to zero after a long time because the particle is assumed to vanish when it hits the boundary (perfectly absorbing boundary), and the chances of the particle hitting the boundary increases over time. However, the rate at which the

probability converges to zero depends largely on the surface area of the disk-shaped region. This can be seen in Figure 3.12a.

So far, we have derived several probability distribution functions for finding a particle performing Brownian motion in a region (that is, Equations (3.8), (3.11), (3.19), and (3.28)). These distribution functions can be fit to data to enable one conclude whether or not an experimental particle of interest is experiencing a restricted motion. To do this, we consider the appropriate probability distribution functions that best model our experimental set-up and collect data such as the initial position of the particle x_0 (r_0 for a disk-shaped region), final position of the particle, its diffusion coefficient D, and final experimental time. These pieces of information can be used in the probability distribution functions to get the distribution of probability for finding the particle in a region, which can then be used together with the final position of the particle to determine whether or not the particle is experiencing a restricted motion.

In the next chapter, we derive probability distribution functions for the case of a partially absorbing boundary and use the distribution function together with maximum likelihood estimation to estimate the rate of absorption on the boundary.

Chapter 4

Partially Absorbing Boundary

In this chapter, we derive probability distribution functions for finding a particle performing Brownian motion in a bounded domain with a partially absorbing boundary. We consider two different geometries: the right half-plane and a disk-shaped region. These distribution functions are used together with maximum likelihood estimation to estimate the rate of absorption on the boundary. In addition, we use the distribution functions to calculate the mean and variance of first passage time for the particle to exit the regions.

4.1 Half-plane problem

Consider a particle performing Brownian motion in the right half-plane with a partially absorbing boundary at $x = 0$. As illustrated in Figure 4.1, if the diffusing particle hits the boundary, it is either absorbed by the boundary (in blue) with a specified probability, or reflected back (in red) into the right half-plane.

Erban and Chapman [4] showed that the partially absorbing boundary is accurately modelled by a Robin boundary condition. If we let Ω be the right half-plane, that is, $\Omega = \{(x,y)|\, 0 \leq x < \infty, -\infty < y < \infty\}$, then the probability of finding the particle at position $\overrightarrow{\mathbf{x}} \in \Omega$ at time t, given that it started at position $\overrightarrow{\mathbf{x}}_0 \in \Omega$ at time

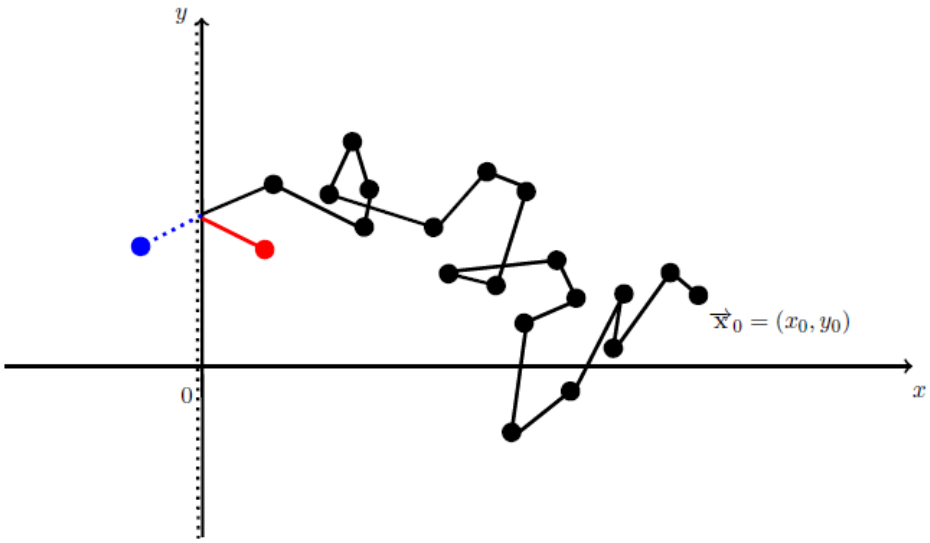

Figure 4.1: A particle performing Brownian motion in the right half-plane with a partially absorbing boundary at $x = 0$.

$t = 0$, $P(\vec{\mathbf{x}}, t|\vec{\mathbf{x}}_0, 0)$ satisfies

$$\begin{aligned} &\frac{\partial P}{\partial t} = D\nabla^2 P, \ \vec{\mathbf{x}} \in \Omega, \ t > 0, \\ &P(\vec{\mathbf{x}}, 0) = \delta(\vec{\mathbf{x}} - \vec{\mathbf{x}}_0), \\ &D\frac{\partial P}{\partial x} = \kappa P, \quad x = 0, \ -\infty < y < \infty, \\ &P \longrightarrow 0, \quad \text{as } x \longrightarrow \infty, \end{aligned} \tag{4.1}$$

where κ is the rate of absorption on the boundary.

Let us rewrite this problem by placing the delta function in the initial condition as a source function in the PDE,

$$\begin{aligned} &\frac{\partial P}{\partial t} = D\nabla^2 P + \delta(x - x_0, y - y_0)\,\delta(t), \quad 0 \le x < \infty, \ -\infty < y < \infty, \ t > 0, \\ &D\partial_n P - \kappa P = 0, \text{ on } x = 0, \ -\infty < y < \infty, \\ &P \equiv 0, \text{ at } t = 0. \end{aligned} \tag{4.2}$$

Let $P = G_f + \widehat{G}$, where G_f is the free space Green's for the diffusion equation, and $\widehat{G}$ is a function to be determined. Substituting $P = G_f + \widehat{G}$ into the PDE in problem (4.2), we have

$$(G_f + \widehat{G})_t = D\nabla^2(G_f + \widehat{G}) + \delta(x - x_0, y - y_0)\,\delta(t)\,.$$

Rearranging,

$$\frac{\partial G_f}{\partial t} - D\nabla^2 G_f = D\nabla^2 \widehat{G} - \frac{\partial \widehat{G}}{\partial t} + \delta(x - x_0, y - y_0)\,\delta(t),\,.$$

Substituting $P = G_f + \widehat{G}$ into the Robin boundary condition in problem (4.2) gives

$$D\partial_n G_f - \kappa G_f = -D\partial_n \widehat{G} + \kappa \widehat{G}\,.$$

Therefore, problem (4.2) becomes

$$\begin{aligned} \frac{\partial G_f}{\partial t} - D\nabla^2 G_f = D\nabla^2 \widehat{G} - \frac{\partial \widehat{G}}{\partial t} + \delta(x - x_0, y - y_0)\,\delta(t), \quad 0 \le x < \infty, \\ -\infty < y < \infty,\ t > 0, \\ D\partial_n G_f - \kappa G_f = -D\partial_n \widehat{G} + \kappa \widehat{G},\ \text{on } x = 0,\ -\infty < y < \infty, \\ G_f \equiv 0,\ \text{at } t = 0\,. \end{aligned} \tag{4.3}$$

Next, we split this problem into two new problems. The first problem is

$$\begin{aligned} \frac{\partial G_f}{\partial t} - D\nabla^2 G_f = \delta(x - x_0, y - y_0)\,\delta(t), \quad -\infty < x, y < \infty,\ t > 0, \\ G_f \equiv 0, \text{ at } t = 0\,. \end{aligned} \tag{4.4}$$

This is the problem for the free space Green's function for the diffusion equation and the solution is the Green's function we derived earlier in Equation (3.7),

$$G_f = \frac{1}{4\pi D t} \exp\left(-\frac{1}{4Dt}[(x - x_0)^2 + (y - y_0)^2] \right). \tag{4.5}$$

The second problem is

$$\begin{aligned} D\nabla^2\widehat{G} - \frac{\partial \widehat{G}}{\partial t} = 0, \quad 0 \le x < \infty,\ -\infty < y < \infty,\ t > 0, \\ D\partial_n G_f - \kappa G_f = -D\partial_n \widehat{G} + \kappa \widehat{G},\ \text{on } x = 0,\ -\infty < y < \infty, . \end{aligned} \tag{4.6}$$

Here, we shall use the idea of the method of images to choose a solution to the PDE in the problem which contains an unknown function called *the source density function* (see page 478 of [19]). This solution together with the boundary condition will be used to find the suitable source density function. We write

$$\widehat{G} = \frac{1}{4\pi Dt}\, e^{-\frac{1}{4Dt}[(x+x_0)^2+(y-y_0)^2]} + \frac{1}{4\pi Dt}\int_{-\infty}^{-x_0} \gamma(s)\, e^{-\frac{1}{4Dt}[(x-s)^2+(y-y_0)^2]} \mathrm{d}s\,, \tag{4.7}$$

where $\gamma(s)$ is the source density function, and it is assumed to decay fast enough at infinity such that the integral converges and differentiation under the integral is possible. In the Robin boundary condition $D\partial_n G - \kappa G = 0$, if $\kappa = 0$, we have the Neumann boundary condition, $\partial_n G = 0$, and so we expect

$$\widehat{G} = \frac{1}{4\pi Dt}\, \exp\left(-\frac{1}{4Dt}[(x+x_0)^2 + (y-y_0)^2]\right).$$

So that

$$\begin{aligned} P(x,y,t|x_0,y_0) = \frac{1}{4\pi Dt}\, \exp\left(-\frac{1}{4Dt}[(x-x_0)^2 + (y-y_0)^2]\right) \\ + \frac{1}{4\pi Dt}\, \exp\left(-\frac{1}{4Dt}[(x+x_0)^2 + (y-y_0)^2]\right), \end{aligned} \tag{4.8}$$

which is the probability distribution function for finding the diffusing particle at position (x,y) at time t when the boundary at $x = 0$ is perfectly reflecting. Therefore, we want the source density function to be zero when $\kappa = 0$. To get this, we need to find the appropriate $\gamma(s)$ such that $\widehat{G}$ satisfies the boundary condition in Problem (4.6).

Substituting G_f and $\widehat{G}$ into the boundary condition in problem (4.6) and sim-

plifying, we have

$$-\frac{2\kappa}{4\pi Dt}\,e^{-\frac{1}{4Dt}[x_0^2+(y-y_0)^2]} = \frac{\kappa}{4\pi Dt}\int_{-\infty}^{-x_0}\gamma(s)\,e^{-\frac{1}{4Dt}[s^2+(y-y_0)^2]}\,\mathrm{d}s - \frac{1}{4\pi t}\int_{-\infty}^{-x_0}\gamma(s)\frac{\partial}{\partial x}\left[e^{-\frac{1}{4Dt}[(x+s)^2+(y-y_0)^2]}\right]\Big|_{x=0}\mathrm{d}s\,.$$

Multiplying through by $4\pi Dt$, and using the fact that $\frac{\partial}{\partial x}\equiv-\frac{\partial}{\partial s}$ on the boundary $(x=0)$, we obtain

$$-2\kappa e^{-\frac{1}{4Dt}[x_0^2+(y-y_0)^2]} = \kappa\int_{-\infty}^{-x_0}\gamma(s)\,e^{-\frac{1}{4Dt}[s^2+(y-y_0)^2]}\,\mathrm{d}s + D\int_{-\infty}^{-x_0}\gamma(s)\frac{\partial}{\partial s}\left[e^{-\frac{1}{4Dt}[s^2+(y-y_0)^2]}\right]\mathrm{d}s\,.$$

Using integration by parts for the second integral on the right hand side,

$$-2\kappa e^{-\frac{1}{4Dt}[x_0^2+(y-y_0)^2]} = \kappa\int_{-\infty}^{-x_0}\gamma(s)\,e^{-\frac{1}{4Dt}[s^2+(y-y_0)^2]}\,\mathrm{d}s + D\gamma(-x_0)\,e^{-\frac{1}{4Dt}[x_0^2+(y-y_0)^2]} - D\int_{-\infty}^{-x_0}\gamma'(s)e^{-\frac{1}{4Dt}[s^2+(y-y_0)^2]}\,\mathrm{d}s\,,\quad\left(\gamma'(s)\equiv\frac{\partial\gamma(s)}{\partial s}\right).$$

Simplifying and collecting the integrals together, we have

$$(2\kappa+D\gamma(-x_0))\,e^{-\frac{1}{4Dt}[x_0^2+(y-y_0)^2]} = (D\gamma'(s)-\kappa\gamma(s))\int_{-\infty}^{-x_0}e^{-\frac{1}{4Dt}[s^2+(y-y_0)^2]}\,\mathrm{d}s\,.$$

We notice that for this to hold, we must have $D\gamma'(s)-\kappa\gamma(s)=0$ and $2\kappa+D\gamma(-x_0)=0$, for $s<-x_0$. Therefore, we have the initial value problem

$$D\gamma'(s)-\kappa\gamma(s)=0\,,\quad s<-x_0\,,$$
$$D\gamma(-x_0)=-2\kappa\,.$$

Solving this initial value problem, we obtain $\gamma(s)=\frac{-2\kappa}{D}\exp\left(\frac{\kappa}{D}(x_0+s)\right)$. Substituting for $\gamma(s)$ in Equation (4.7) gives

$$\widehat{G}=\frac{1}{4\pi Dt}\,e^{-\frac{1}{4D\sigma}[(x+x_0)^2+(y-y_0)^2]}-\frac{2\kappa}{4\pi D^2t}\int_{-\infty}^{-x_0}e^{\frac{\kappa}{D}(x_0+s)}\,e^{-\frac{1}{4Dt}[(x-s)^2+(y-y_0)^2]}\,\mathrm{d}s\,.$$

Substituting G_f and $\widehat{G}$ into $P = G_f + \widehat{G}$, we have

$$P(\overrightarrow{\mathbf{x}},t) = \frac{1}{4\pi Dt}\left[e^{-\frac{1}{4Dt}[(x-x_0)^2+(y-y_0)^2]} + e^{-\frac{1}{4Dt}[(x+x_0)^2+(y-y_0)^2]}\right] - \frac{\kappa}{2\pi D^2 t}\int_{-\infty}^{-x_0} e^{\frac{\kappa}{D}(x_0+s)}\, e^{-\frac{1}{4Dt}[(x-s)^2+(y-y_0)^2]}\,\mathrm{d}s\,.$$

Evaluating the integral, we get

$$P(\overrightarrow{\mathbf{x}},t) = \frac{1}{4\pi Dt}\left[e^{-\frac{1}{4Dt}[(x-x_0)^2+(y-y_0)^2]} + e^{-\frac{1}{4Dt}[(x+x_0)^2+(y-y_0)^2]}\right] - \frac{\kappa}{\pi D(x+x_0)+2\pi Dt\,\kappa}\left(e^{-\frac{1}{4Dt}[(x+x_0)^2+(y-y_0)^2]}\right)\,. \tag{4.9}$$

This is the probability distribution function for finding a particle performing Brownian motion in the right half-plane at position $\overrightarrow{\mathbf{x}}$ at time t, given that it started from position $\overrightarrow{\mathbf{x}}_0$ at time $t = 0$ and that there is a partially absorbing boundary at $x = 0$.

We shall integrate this function over the right half-plane to obtain the probability distribution function for finding the particle in the right half-plane at any given time t, that is

$$\Gamma(t|x_0) = \int_{-\infty}^{\infty}\int_{0}^{\infty} P(x,y,t|x_0,y_0)\,\mathrm{d}x\,\mathrm{d}y\,.$$

Substituting $P(\overrightarrow{\mathbf{x}},t)$ as given in Equation (4.9) into this equation,

$$\Gamma(t|x_0) = \frac{1}{4\pi Dt}\int_{-\infty}^{\infty}\int_{0}^{\infty}\left[e^{-\frac{1}{4Dt}[(x-x_0)^2+(y-y_0)^2]} + e^{-\frac{1}{4Dt}[(x+x_0)^2+(y-y_0)^2]}\right]\,\mathrm{d}x\,\mathrm{d}y - \int_{-\infty}^{\infty}\int_{0}^{\infty}\frac{\kappa}{\pi D(x+x_0)+2\pi Dt\,\kappa}\left[e^{-\frac{1}{4Dt}[(x+x_0)^2+(y-y_0)^2]}\right]\,\mathrm{d}x\,\mathrm{d}y\,.$$

Evaluating the integrals in the first term, we have

$$\Gamma(t|x_0) = \frac{1}{2}\left[\operatorname{erfc}\left(-\frac{x_0}{\sqrt{4Dt}}\right) + \operatorname{erfc}\left(\frac{x_0}{\sqrt{4Dt}}\right)\right] - \int_0^{\infty}\frac{\sqrt{4\pi Dt}\,\kappa}{\pi D(x+x_0)+2\pi Dt\,\kappa}\left(e^{-\frac{1}{4Dt}(x+x_0)^2}\right)\,\mathrm{d}x\,.$$

Since $\frac{1}{2}\left[\text{erfc}\left(-\frac{x_0}{\sqrt{4Dt}}\right)+\text{erfc}\left(\frac{x_0}{\sqrt{4Dt}}\right)\right]=1$, we can write

$$\Gamma(t|x_0)=1-\int_0^\infty \frac{\sqrt{4\pi Dt}\,\kappa}{\pi D(x+x_0)+2\pi Dt\,\kappa}\left(e^{-\frac{1}{4Dt}(x+x_0)^2}\right)\,\mathrm{d}x\ .$$

Let $\Gamma(t|x_0)=1-\sqrt{4\pi Dt}\,\kappa I$, where

$$I=\int_0^\infty \frac{1}{\pi D(x+x_0)+2\pi Dt\,\kappa}\left(e^{-\frac{1}{4Dt}(x+x_0)^2}\right)\,\mathrm{d}x.$$

Rewriting I, we have

$$I=\frac{1}{\pi D}\int_0^\infty \left(\frac{1}{x+(x_0+2t\,\kappa)}\right)e^{-\frac{1}{4Dt}(x+x_0)^2}\,\mathrm{d}x.$$

We notice that this integral does not converge, therefore, to evaluate the integral analytically, we Taylor expand the fraction in the integrand near $x=0$ to have

$$I\simeq\frac{1}{D\pi}\int_0^\infty\left(\frac{1}{(x_0+2t\,\kappa)}-\frac{x}{(x_0+2t\,\kappa)^2}+\frac{x^2}{(x_0+2t\,\kappa)^3}+\ldots\right)e^{-\frac{1}{4Dt}(x+x_0)^2}\,\mathrm{d}x\ .$$

$$I\simeq\frac{1}{D\pi(x_0+2t\,\kappa)}\left[\int_0^\infty e^{-\frac{1}{4Dt}(x+x_0)^2}\,\mathrm{d}x-\frac{1}{(x_0+2t\,\kappa)}\int_0^\infty x\,e^{-\frac{1}{4Dt}(x+x_0)^2}\,\mathrm{d}x+\ldots\right].$$

Evaluating the integrals, we obtain

$$\begin{aligned}I\simeq\frac{1}{D\pi(x_0+2t\,\kappa)}&\left[\frac{\sqrt{4\pi Dt}}{2}\text{erfc}\left(\frac{x_0}{\sqrt{4Dt}}\right)\right.\\&\left.-\frac{1}{2(x_0+2t\,\kappa)}\left(4Dt\,e^{(-\frac{x_0^2}{4Dt})}-\sqrt{4\pi Dt}\,x_0\,\text{erfc}\left(\frac{x_0}{\sqrt{4Dt}}\right)\right)+\ldots\right].\end{aligned}$$

Therefore,

$$\begin{aligned}I\simeq\frac{1}{D\pi(x_0+2t\,\kappa)}&\left[\frac{\sqrt{4\pi Dt}}{2}\text{erfc}\left(\frac{x_0}{\sqrt{4Dt}}\right)\right.\\&\left.-\frac{1}{2(x_0+2t\,\kappa)}\left(4Dt\,e^{(-\frac{x_0^2}{4Dt})}-\sqrt{4\pi Dt}\,x_0\,\text{erfc}\left(\frac{x_0}{\sqrt{4Dt}}\right)\right)\right].\end{aligned}\tag{4.10}$$

It is important to point out that this solution is valid for $1 < |x_0 + 2\kappa t|$. Thus

$$\Gamma(t|x_0) = 1 - \frac{\sqrt{4\pi Dt}\,\kappa}{\pi D(x_0+2t\kappa)}\left[\frac{\sqrt{4\pi Dt}}{2}\operatorname{erfc}\left(\frac{x_0}{\sqrt{4Dt}}\right)\right.$$
$$\left. -\frac{1}{2(x_0+2t\kappa)}\left(4Dt\,\exp\left(-\frac{x_0^2}{4Dt})\right) - \sqrt{4\pi Dt}\,x_0\operatorname{erfc}\left(\frac{x_0}{\sqrt{4Dt}}\right)\right)\right].$$

Simplifying, we have the probability distribution function for finding the particle in the right half-plane at time t as

$$\Gamma(t|x_0) = 1 - \left[\left(1+\frac{x_0}{(x_0+2t\kappa)}\right)\frac{2t\,\kappa}{(x_0+2t\kappa)}\operatorname{erfc}\left(\frac{x_0}{\sqrt{4Dt}}\right)\right.$$
$$\left. -\frac{4(Dt)^{3/2}\kappa}{\sqrt{\pi}D(x_0+2t\kappa)^2}\exp\left(-\frac{x_0^2}{4Dt}\right)\right]. \tag{4.11}$$

where κ is the rate of absorption on the boundary, x_0 is the initial position of the particle, and D is its diffusion coefficient.

We observe from the Robin boundary condition $D\frac{\partial P}{\partial x} = \kappa P$ that if $\kappa = 0$, the boundary condition becomes a perfectly reflecting (Neumann) boundary condition, $\frac{\partial P}{\partial x} = 0$. And if we set $\kappa = 0$ in the probability distribution function in Equation (4.11), we have $\Gamma(t|x_0) = 1$ which corresponds to the probability that the particle is in the right half-plane at time t, given that the boundary at $x = 0$ is perfectly reflecting. This is logical because the particle will remain in the region for all time since the boundary is perfectly reflecting.

On the other hand, if we take the limit of the Robin boundary condition as κ tends to infinity, the boundary condition becomes the perfectly absorbing boundary condition, $P = 0$. Also, taking the limit of the distribution function in Equation (4.11) as κ tends to infinity, we have

$$\Gamma(t|x_0) = 1 - \operatorname{erfc}\left(\frac{x_0}{\sqrt{4Dt}}\right) = \frac{1}{2}\left[\operatorname{erfc}\left(-\frac{x_0}{\sqrt{4Dt}}\right) - \operatorname{erfc}\left(\frac{x_0}{\sqrt{4Dt}}\right)\right],$$

which is the same as the probability distribution function derived in Chapter 3 (Equation (3.19)) for finding a diffusing particle in the right half-plane, where the boundary at $x = 0$ is perfectly absorbing. This shows that the probability distri-

bution function for a partially absorbing boundary is a weighted average of the distribution functions for an absorbing boundary and that of a reflecting boundary.

Next, we simulate trajectories with the particle based simulation software [2], calculate the probability of finding a diffusing particle in the right half-plane from the simulation, and compare the result to that of the probability distribution function in Equation (4.11). To calculate the probability of finding a particle performing Brownian motion in a region at a specific time with simulation, we simulate several trajectories that all start at the same point, count the number of trajectories that are remaining in the region at each time step and divide by the initial number of trajectories. This gives the probability that a single trajectory that started a Brownian motion at that point is still in the region at each time step. We specify a particular rate of absorption on the boundary κ, and use the relation in Equation (2.9) to get the corresponding probability of absorption on the boundary which is then used for the simulation.

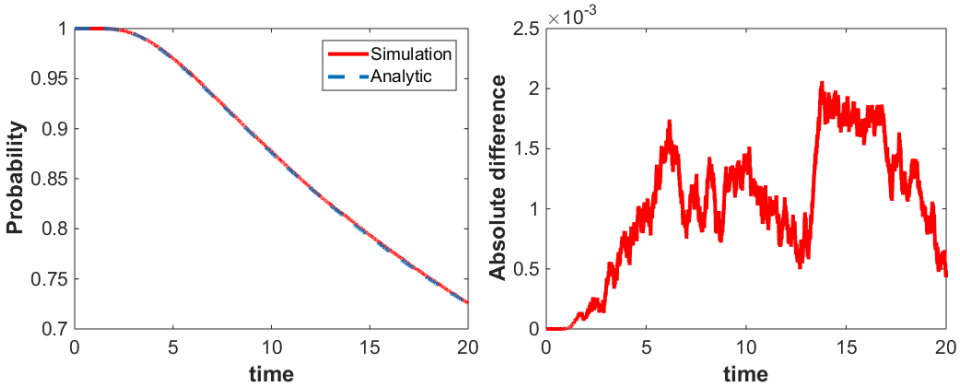

(a) Probability of finding the particle in the right half-plane.

(b) Absolute difference of the analytic and simulated result.

Figure 4.2: The comparison of the probability of finding the particle in the right half-plane obtained from the simulation and that of the probability distribution function in Equation (4.11).

Figure 4.2a shows a comparison of the probability that the particle performing Brownian motion in the right half-plane is still in the region at time t, calculated from simulation, and that of the probability distribution function in Equation (4.11), while Figure 4.2b shows the absolute difference of the two results. For the

result obtained from simulation, we averaged over 10 different simulations using $10,000$ particles for each simulation, with $\kappa = 0.5$ which corresponds to probability of absorption $\mathbb{P} = 0.044$, $D = 0.1$, and $x_0 = 2$. We can see from this figure that the two result agree to a large extent.

Let us calculate the mean and variance of first passage time for the diffusing particle to exit the right half-plane. First, we notice that the probability that the particle is still in the right half-plane at time t given that it started at point x_0 is equivalent to the probability that the time it takes the particle to be absorbed by the boundary given that it started from x_0 is greater than t, that is,

$$\Gamma(t|x_0) = \int_t^\infty \Psi(\tau|x_0)\,\mathrm{d}\tau\,, \tag{4.12}$$

where $\Psi(\tau|x_0)$ is the probability distribution function for the first passage time for the particle to exit the region. From Equation (4.12), we have

$$\Psi(t|x_0) = -\frac{\partial}{\partial t}\Gamma(t|x_0)\,. \tag{4.13}$$

Substituting $\Gamma(t|x_0)$ as given in Equation (4.11) into Equation (4.13), we obtain

$$\begin{aligned}\Psi(t|x_0) = \frac{4\kappa x_0^2}{(x_0+2t\kappa)^3}\operatorname{erfc}\left(\frac{x_0}{\sqrt{4Dt}}\right) + \left[x_0^2 + 2t\kappa\left(x_0 - \frac{3D}{\kappa} + \frac{8Dt}{(x_0+2t\kappa)}\right)\right] \\ \times \frac{\kappa}{\sqrt{D\pi t}(x_0+2t\kappa)^2}\exp\left(-\frac{x_0^2}{4Dt}\right)\,.\end{aligned} \tag{4.14}$$

Let $\Pi(t|x_0)$ be the mean first passage time for the particle to exit the region, given that it started at x_0. Since the first moment of the probability distribution for the first passage time is the mean first passage time, we have

$$\Pi(t|x_0) = \int_0^\infty t\,\Psi(t|x_0)\,\mathrm{d}t\,. \tag{4.15}$$

The second moment of the distribution is

$$\Phi(t|x_0) = \int_0^\infty t^2\,\Psi(t|x_0)\,\mathrm{d}t\,. \tag{4.16}$$

Therefore, the variance of first passage time for the particle to exit the region given that it started at x_0 is

$$\mathbf{V}(t|x_0) = \Phi(t|x_0) - \Pi(t|x_0)^2 . \tag{4.17}$$

We substitute Equation (4.14) into Equations (4.15) and (4.16), and evaluate the resulting integrals numerically. These results are then used to compute the mean and variance of first passage time for the particle to exit the right half-plane.

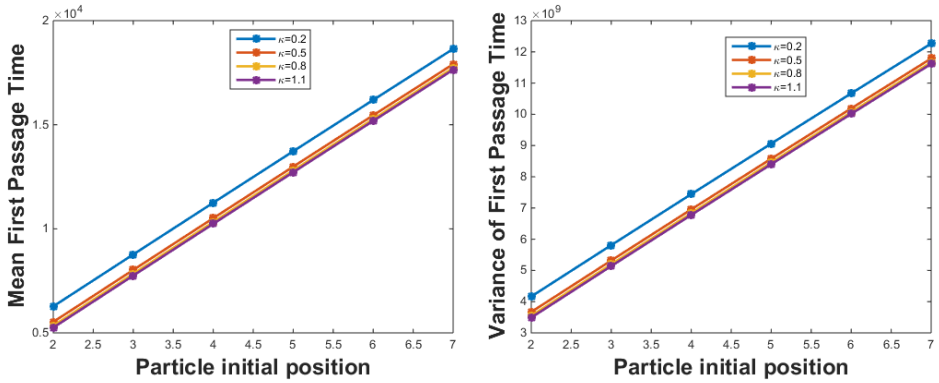

(a) Mean first passage time. **(b)** Variance of first passage time.

Figure 4.3: The mean and variance of first passage time for a particle performing Brownian motion in the right half-plane, with a partially absorbing boundary at $x = 0$.

Figure 4.5 shows the plots of the mean and variance of first passage time for a diffusing particle to exit the right half-plane for different values of κ. We observe from Figure 4.5a that the mean first passage time increases as the initial position of the particle moves farther away from the boundary. This is not surprising because the farther away from the boundary the particle starts, the longer it takes it to reach the boundary. Also we observe that as the rate of absorption on the boundary increases, the mean first passage time decreases. This is because the particle is easily absorbed on the boundary as the rate of absorption on the boundary increases. The mean and variance of first passage time tells us how long we should expect a particle performing Brownian motion in the right half-plane to stay in the region before it gets absorbed by the boundary.

4.2 The disk problem

Suppose the diffusing particle is in a disk-shaped region of radius a with a partially absorbing boundary. Let $\Omega = \{(r,\theta)\,|\,0 < r \le a, 0 \le \theta \le 2\pi\}$, then the probability of finding the particle at position $\overrightarrow{\mathbf{x}} = (r,\theta)$ at time t, given that it started at position $\overrightarrow{\mathbf{x}}_0 = (r_0,\theta_0)$ at time $t = 0$ satisfies

$$\begin{aligned} &\frac{\partial P}{\partial t} = D\nabla^2 P,\ \overrightarrow{\mathbf{x}} = (r,\theta) \in \Omega,\ t > 0\,, \\ &\quad D\frac{\partial P}{\partial n} = -\kappa P, \quad \text{on } \partial\Omega\,, \\ &\quad P \text{ is finite as } r \longrightarrow 0\,, \\ &\quad P(\overrightarrow{\mathbf{x}},0) = \delta(\overrightarrow{\mathbf{x}} - \overrightarrow{\mathbf{x}}_0)\,. \end{aligned} \tag{4.18}$$

where κ is the rate of absorption on the boundary, and D is the diffusion coefficient of the particle.

We shall solve this problem using separation of variables. First, let us rewrite the problem by writing the delta function in the initial condition as a forcing in the PDE, that is,

$$\begin{aligned} \frac{\partial P}{\partial t} =& D\left(\frac{1}{r}\frac{\partial P}{\partial r} + \frac{\partial^2 P}{\partial r^2}\right) + \frac{\delta(r-r_0)\delta(t)}{2\pi r}, \quad 0 < r \le a\,,\ t > 0\,, \\ & D\frac{\partial P}{\partial r} = -\kappa P,\ \text{on } r = a\,, \\ & P \text{ is finite as } r \longrightarrow 0\,, \\ & P \equiv 0,\ \text{at } t = 0\,. \end{aligned} \tag{4.19}$$

It is important to note that we have assumed that there is uniformity in the θ direction so that the problem is independent of θ.

From the problem in Equation (4.19), we consider the homogeneous part of the PDE

$$\frac{\partial P}{\partial t} = D\left(\frac{1}{r}\frac{\partial P}{\partial r} + \frac{\partial^2 P}{\partial r^2}\right), \tag{4.20}$$

together with the following boundary conditions

$$\begin{aligned} &D\frac{\partial P}{\partial r} = -\kappa P, \text{ on } r = a, \\ &P \text{ is finite as } r \longrightarrow 0. \end{aligned} \tag{4.21}$$

Let $P(r,t) = R(r)T(t)$, then from Equations (4.20) and (4.21), we have

$$\begin{aligned} R(r)\frac{\mathrm{d}}{\mathrm{d}t}T(t) &= D\left(\frac{1}{r}T(t)\frac{\mathrm{d}}{\mathrm{d}r}R(r) + T(t)\frac{\mathrm{d}^2}{\mathrm{d}r^2}R(r)\right), \\ D\frac{\mathrm{d}}{\mathrm{d}r}R(r) &= -\kappa R(r) \text{ on } r = a, \\ R(r) &\text{ is finite as } r \longrightarrow 0. \end{aligned} \tag{4.22}$$

Let us consider

$$\frac{1}{DT(t)}\frac{\mathrm{d}}{\mathrm{d}t}T(t) = \frac{1}{R(r)}\left(\frac{1}{r}\frac{\mathrm{d}}{\mathrm{d}r}R(r) + \frac{\mathrm{d}^2}{\mathrm{d}r^2}R(r)\right).$$

For this to hold, it must equal a constant, that is

$$\frac{1}{DT(t)}\frac{\mathrm{d}}{\mathrm{d}t}T(t) = \frac{1}{R(r)}\left(\frac{1}{r}\frac{\mathrm{d}}{\mathrm{d}r}R(r) + \frac{\mathrm{d}^2}{\mathrm{d}r^2}R(r)\right) = -\lambda^2. \tag{4.23}$$

where λ is a constant.

Therefore, we have the following equations

$$\frac{1}{DT(t)}\frac{\mathrm{d}}{\mathrm{d}t}T(t) = -\lambda^2 \qquad \text{and} \qquad \frac{1}{R(r)}\left(\frac{1}{r}\frac{\mathrm{d}}{\mathrm{d}r}R(r) + \frac{\mathrm{d}^2}{\mathrm{d}r^2}R(r)\right) = -\lambda^2. \tag{4.24}$$

Consider

$$\frac{1}{R(r)}\left(\frac{1}{r}\frac{\mathrm{d}}{\mathrm{d}r}R(r) + \frac{\mathrm{d}^2}{\mathrm{d}r^2}R(r)\right) = -\lambda^2.$$

Multiplying through by $r^2R(r)$ and re-arranging, we have the Bessel equation

$$r^2R''(r) + rR'(r) + r^2\lambda^2R(r) = 0.$$

And the solution of this equation is

$$R(r) = AJ_0(\lambda r) + BY_0(\lambda r)\,,$$

where $J_0(z)$ is the Bessel function of the first kind of order zero, and $Y_0(z)$ is the Bessel function of the second kind of order zero.

To satisfy the condition that $R(r)$ is finite as r tends to zero, we must have $B = 0$ because $Y_0(\lambda r)$ is unbounded as r tends to zero. Therefore,

$$R(r) = AJ_0(\lambda r)\,.$$

Imposing the second boundary condition in Equation (4.22), we have

$$D\frac{\mathrm{d}}{\mathrm{d}r}J_0(\lambda r) = -\kappa J_0(\lambda r)\,,\ \text{on } r = a\,.$$

And this gives the following equation for the eigenvalues of the system

$$\kappa J_0(\lambda a) + D\lambda J_1(\lambda a) = 0. \tag{4.25}$$

Let β_m be the m^{th} zero of the eigenvalue equation, then $\lambda_m = \frac{\beta_m}{a}$. Therefore, we have the eigen condition

$$a\kappa J_0(\beta_m) + D\beta_m J_1(\beta_m) = 0, \qquad m = 1,2,3,\ldots \tag{4.26}$$

Without loss of generality, let $A_m = 1$ for all m. Then

$$R_m(r) = J_0(\lambda_m r) = J_0\left(\frac{\beta_m}{a}r\right), \qquad m = 1,2,3,\ldots \tag{4.27}$$

Recall that $P(r,t) = R(r)T(t)$. This implies that $P_m(r,t) = R_m(r)T_m(t)$ for all m. Therefore, using the principle of superposition, we have

$$P(r,t) = \sum_{m=1}^{\infty} T_m(t)\,R_m(r) = \sum_{m=1}^{\infty} T_m(t)\,J_0\left(\frac{\beta_m}{a}r\right). \tag{4.28}$$

Now, let

$$\sum_{m=1}^{\infty} H_m(t) R_m(r) = \frac{\delta(r-r_0)\delta(t)}{2\pi r}, \tag{4.29}$$

Substituting $R_m(r)$ into this equation, and multiplying through by r, we have

$$\sum_{m=1}^{\infty} r H_m(t) J_0\left(\frac{\beta_m}{a} r\right) = \frac{\delta(r-r_0)\delta(t)}{2\pi}.$$

Multiplying both sides by $J_0\left(\frac{\beta_n}{a} r\right)$, and integrating with respect to r from 0 to a,

$$\sum_{m=1}^{\infty} H_m(t) \int_0^a r J_0\left(\frac{\beta_m}{a} r\right) J_0\left(\frac{\beta_n}{a} r\right) \mathrm{d}r = \frac{\delta(t)}{2\pi} \int_0^a J_0\left(\frac{\beta_n}{a} r\right) \delta(r-r_0)\,\mathrm{d}r.$$

By the orthogonality property of Bessel functions,

$$\int_0^a r J_0(\frac{\beta_m}{a} r) J_0\left(\frac{\beta_n}{a} r\right) \mathrm{d}r = 0, \quad m \neq n.$$

And so, we have

$$H_m(t) \int_0^a r J_0^2\left(\frac{\beta_m}{a} r\right) \mathrm{d}r = \frac{\delta(t)}{2\pi} J_0\left(\frac{\beta_m}{a} r_0\right).$$

But

$$\int_0^a r J_0^2\left(\frac{\beta_m}{a} r\right) \mathrm{d}r = \frac{a^2}{2}\left[J_0^2(\beta_m) + J_1^2(\beta_m)\right].$$

Therefore,

$$H_m(t) = \frac{J_0\left(\frac{\beta_m}{a} r_0\right)}{\pi a^2\left[J_0^2(\beta_m) + J_1^2(\beta_m)\right]} \delta(t). \tag{4.30}$$

From Equation (4.19), we have

$$\frac{\partial P}{\partial t} = D\left(\frac{1}{r}\frac{\partial G}{\partial r} + \frac{\partial^2 G}{\partial r^2}\right) + \frac{\delta(r-r_0)\delta(t)}{2\pi r}, \tag{4.31}$$

Substituting Equations (4.28) and (4.29) into Equation (4.31),

$$\begin{aligned}\sum_{m=1}^{\infty} T_m'(t)\,R_m(r) &= D\left[\frac{1}{r}\sum_{m=1}^{\infty} T_m(t)\,R_m'(r) + \sum_{m=1}^{\infty} T_m(t)\,R_m''(r)\right] + \sum_{m=1}^{\infty} H_m(t)\,R_m(r)\,,\\ &= D\left[\sum_{m=1}^{\infty} T_m(t)\,\left(\frac{1}{r}R_m'(r) + R_m''(r)\right)\right] + \sum_{m=1}^{\infty} H_m(t)\,R_m(r)\,.\end{aligned} \tag{4.32}$$

From the Bessel equation, we have

$$R_m''(r) + \frac{1}{r}R_m'(r) = -\lambda_m^2 R_m(r)\,.$$

Therefore, Equation (4.32) becomes

$$\sum_{m=1}^{\infty} T_m'(t)\,R_m(r) = \sum_{m=1}^{\infty} \left(-D\lambda_m^2 T_m(t) + H_m(t)\right) R_m(r)\,.$$

And from this equation, we have

$$T_m'(t) = -D\lambda_m^2 T_m(t) + H_m(t)\,.$$

Substituting $H_m(t)$ as given in Equation (4.30) into this equation,

$$T_m'(t) + D\lambda_m^2 T_m(t) = \frac{J_0\left(\frac{\beta_m}{a}r_0\right)}{\pi a^2\left[J_0^2(\beta_m) + J_1^2(\beta_m)\right]}\delta(t)\,.$$

This is a first order linear ODE. We shall solve this ODE using the integrating factor method. The integrating factor is $\exp\left(D\lambda_m^2 t\right)$, therefore,

$$\frac{\mathrm{d}}{\mathrm{d}t}\left[\exp\left(D\lambda_m^2 t\right) T_m(t)\right] = \frac{J_0\left(\frac{\beta_m}{a}r_0\right)}{\pi a^2\left[J_0^2(\beta_m) + J_1^2(\beta_m)\right]}\delta(t)\exp\left(D\lambda_m^2 t\right)\,.$$

Integrating both sides of the equation with respect to t,

$$\exp\left(D\lambda_m^2 t\right) T_m(t) = \frac{J_0\left(\frac{\beta_m}{a} r_0\right)}{\pi a^2 \left[J_0^2(\beta_m) + J_1^2(\beta_m)\right]} \int_0^t \delta(s) \exp\left(D\lambda_m^2 s\right) \, \mathrm{d}s + E_m \,, \quad (4.33)$$

where E_m are constants of integration.

We shall use the initial condition $P(r,0) = 0$ to find the constants E_m. We have

$$P(r,0) = \sum_{m=1}^{\infty} T_m(0) R_m(r) \,.$$

Setting $t = 0$ in Equation (4.33), we get $T_m(0) = E_m$. And substituting this into $P(r,0)$ gives

$$P(r,0) = \sum_{m=1}^{\infty} T_m(0) R_m(r) = \sum_{m=1}^{\infty} E_m R_m(r) \,.$$

Using the orthogonality property of Bessel functions and the fact that $P(r,0) = 0$, we have that $E_m = 0$ for all m. Therefore, from Equation (4.33) we obtain

$$T_m(t) = \frac{J_0\left(\frac{\beta_m}{a} r_0\right)}{\pi a^2 \left[J_0^2(\beta_m) + J_1^2(\beta_m)\right]} \exp\left(-D\lambda_m^2 t\right) .$$

Substituting $\lambda_m = \frac{\beta_m}{a}$ and $J_1(\beta_m) = \frac{\kappa}{D}\lambda_m J_0(\beta_m)$, we have

$$T_m(t) = \frac{D^2 \beta_m^2}{a^2 \pi} \frac{J_0\left(\frac{\beta_m}{a} r_0\right)}{(D^2\beta_m^2 + \kappa^2 a^2) J_0^2(\beta_m)} \exp\left(-D\frac{\beta_m^2}{a^2} t\right) . \quad (4.34)$$

Substituting $T_m(t)$ and $R_m(r)$ into Equation (4.28), we have

$$P(r,t|r_0) = \frac{D^2}{a^2 \pi} \sum_{m=1}^{\infty} \frac{\beta_m^2 J_0\left(\frac{\beta_m}{a} r_0\right) J_0\left(\frac{\beta_m}{a} r\right)}{(D^2\beta_m^2 + \kappa^2 a^2) J_0^2(\beta_m)} \exp\left(-D\frac{\beta_m^2}{a^2} t\right) . \quad (4.35)$$

This is the probability distribution function for finding a particle performing Brownian motion in a disk-shaped region of radius a, at a distance r from the center of the region at time t, given that it started at a distance r_0 from the center, and that

the region has a partially absorbing boundary.

Lastly, we integrate Equation (4.35) to get the probability distribution function for finding the particle inside the disk-shaped region at time t.

$$\Gamma(t|r_0) = \frac{D^2}{a^2\pi} \sum_{m=1}^{\infty} \frac{\beta_m^2 J_0\left(\frac{\beta_m}{a} r_0\right)}{(D^2\beta_m^2 + \kappa^2 a^2) J_0^2(\beta_m)} \exp\left(-D\frac{\beta_m^2}{a^2} t\right) \int_0^{2\pi} \int_0^a r J_0\left(\frac{\beta_m}{a} r\right) \mathrm{d}r\,\mathrm{d}\theta\,.$$

$$\Gamma(t|r_0) = 2D^2 \sum_{m=1}^{\infty} \frac{\beta_m J_0\left(\frac{\beta_m}{a} r_0\right) J_1(\beta_m)}{(D^2\beta_m^2 + \kappa^2 a^2) J_0^2(\beta_m)} \exp\left(-D\frac{\beta_m^2}{a^2} t\right)\,. \tag{4.36}$$

Figure 4.4a shows the comparison of the probability of finding a diffusing particle in a disk-shaped region of radius $a = 5$ calculated from simulation and that of the probability distribution function in Equation (4.36), while Figure 4.4b shows the absolute difference of the two results. For the simulated result, we averaged over 10 different simulations each with $10,000$ particles starting from a distance $r_0 = 2$ away the center of the region, with diffusion coefficient $D = 0.1$, and the rate of absorption on the boundary $\kappa = 0.85$. We observe from theses figures that the simulated result is in accordance with that obtained from the probability distribution function.

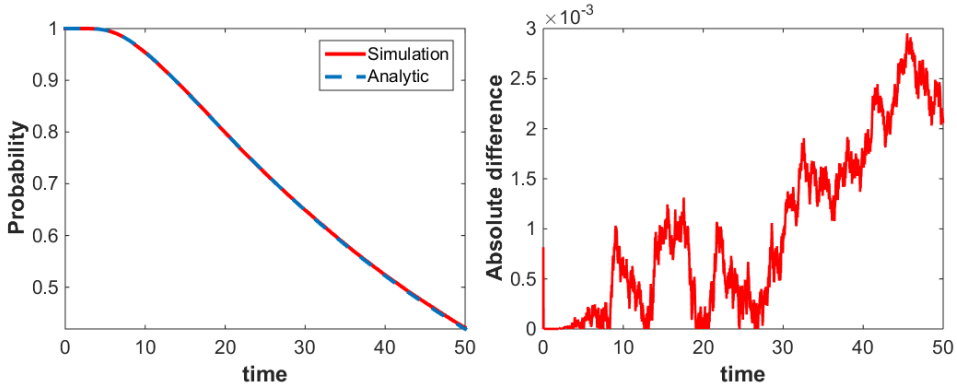

(a) Probability of finding the particle in the disk-shaped region.

(b) Absolute difference of the analytic and numerical result.

Figure 4.4: The comparison of the probability of finding a particle in the disk-shaped region calculated from simulation and that of the probability distribution function in Equation (4.36).

Similar to the right half-plane problem, we want to calculate the mean and variance of first passage time for a particle performing Brownian motion in a disk-shaped region to exit the region. Substituting Equation (4.36) into Equation (4.13), we obtain the distribution function for first passage time for a diffusing particle in the disk-shaped region,

$$\Psi(t|r_0) = \frac{2D^3}{a^2} \sum_{m=1}^{\infty} \frac{\beta_m^3 J_0\left(\frac{\beta_m}{a} r_0\right) J_1(\beta_m)}{(D^2\beta_m^2 + \kappa^2 a^2) J_0^2(\beta_m)} \exp\left(-D\frac{\beta_m^2}{a^2} t\right). \tag{4.37}$$

Using Equations (4.15), (4.16), and (4.17), we can get the mean and variance of first passage time for the particle. We substitute Equation (4.37) into the integrals in Equations (4.15) and (4.16), and evaluate the resulting integrals numerically to get the mean and the second moment of the distribution. These results are then used in Equation (4.17) to compute the variance of first passage time for the particle. Figure 4.5 shows the plots of the mean and variance of first passage time for a particle performing Brownian motion in a disk-shaped region of radius $a = 7$, with a partially absorbing boundary.

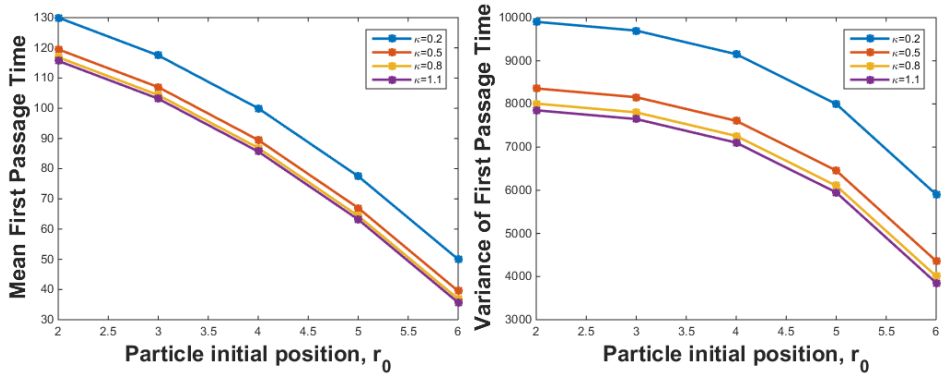

(a) Mean first passage time. **(b)** Variance of first passage time.

Figure 4.5: The mean and variance of first passage time for a particle performing Brownian motion in a disk-shaped region with a partially absorbing boundary.

For this figure, we used $D = 0.1$, and varied the rate of absorption on the boundary and the initial position of the particle. It is important to note that the initial

position of the particle r_0 is the distance of the particle from the centre of the disk-shaped region. As we would expect, the mean first passage time for the particle to exit the region decreases as the initial position of the particle gets closer to the boundary. This is due to the fact that the time it takes the particle to reach the boundary when it starts close to the boundary is less compared to when the particle starts farther away from the boundary. Also, like in the right half-plane problem, we observe that the mean first passage time decreases as the rate of absorption on the boundary increases. This is because the particle is easily absorbed as the rate of absorption on the boundary gets larger. Unlike the case of a particle in the right half-plane where the mean and variance of first passage time are linear with respect to the initial position of the particle, they are non-linear for this case, and this is as a result of the geometry of the region.

4.2.1 Estimating the rate of absorption on the boundary

In this section, we present a mathematical technique for estimating the rate of absorption on a partially absorbing boundary using the probability distribution functions we derived for a particle performing Brownian motion in regions with partially absorbing boundary together with maximum likelihood estimation.

First, let us derive the likelihood function. We define the likelihood function of having the parameter κ given some observations as

$$\ell(\kappa|\text{Observations}) = \mathbf{P}(\text{Observations};\kappa)\,. \tag{4.38}$$

where $\mathbf{P}(\text{Observations};\kappa)$ is the probability of having these observations with parameter κ. There are only two possible observations here;

- the diffusing particle has been absorbed by the boundary at time t
- the particle is still in the region at time t

Let Σ be our region of interest. Suppose there are $n+m$ identical particles starting a Brownian motion at a specific point in Σ at time $t=0$, the motion of each particle is independent. Let $\mathbf{P}(\text{Particle in }\Sigma;\kappa)$ be the probability that a particle is still in the region of interest at time t given that κ is a parameter, and let $\mathbf{P}(\text{Particle absorbed};\kappa)$ be the probability that a particle has been absorbed by the

boundary at time t. Then, the probability of having the observations that n particles are still remaining in the region, while m of them have been absorbed by the boundary at time t, given that κ is a parameter is

$$\mathbf{P}(\text{Observations};\kappa) = \mathbf{P}(\text{Particle is in } \Sigma;\kappa)^n \times \mathbf{P}(\text{Particle absorbed};\kappa)^m .$$

But $\mathbf{P}(\text{Particle absorbed};\kappa) = 1 - \mathbf{P}(\text{Particle is in } \Sigma;\kappa)$, therefore,

$$\mathbf{P}(\text{Observations};\kappa) = \mathbf{P}(\text{Particle is in } \Sigma;\kappa)^n \times (1 - \mathbf{P}(\text{Particle is in } \Sigma;\kappa))^m .$$

And so, the likelihood function is

$$\ell(\kappa|\text{Observations}) = \mathbf{P}(\text{Particle is in } \Sigma;\kappa)^n \times (1 - \mathbf{P}(\text{Particle is in } \Sigma;\kappa))^m ,$$

where n is the number of particles left in the region of interest, and m is the number of particles that were absorbed by the boundary after a specific time.

Thus, the likelihood function can be written as

$$\ell(\kappa|\text{Observations}) = (\Gamma(t|x_0))^n \times (1 - (\Gamma(t|x_0))^m , \tag{4.39}$$

where $\Gamma(t|x_0)$ is the probability distribution function for finding a particle in the region of interest at time t given that it started from the point x_0 in the region. That is, Equation (4.11) for the right half-plane problem, and Equation (4.36) for the disk problem.

We need to maximize the likelihood function with respect to κ, and the κ value that maximizes this function is the most probable rate of absorption on the boundary with respect to the observations or data.

To validate this idea, we simulate trajectories using the particle based simulation software [2] with a specific rate of absorption on the boundary, collect data from the simulation in terms of the number of trajectories remaining in the region of interest and those that have been absorbed by the boundary after a specified time. The data collected are used in the likelihood function in Equation (4.39), and then the resulting function is maximized with respect to κ to recover the rate of absorption used for the simulation.

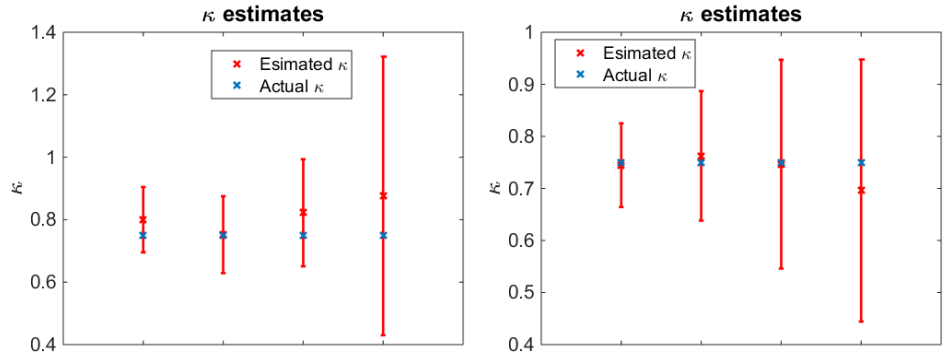

(a) **(b)**

Figure 4.6: Estimates of the rate of absorption on the boundary with standard deviation error bars based on simulated data considering different particle initial positions x_0, for the half-plane problem.

Figure 4.6 shows the result of our estimates of the rate of absorption on the boundary with standard deviation error bars, based on simulated data for a particle performing Brownian motion in the right half-plane. Here, we used a fixed rate of absorption $\kappa = 0.75$, diffusion coefficient $D = 0.1$, and vary the initial position of the particles. For each initial position, we simulate $10,000$ trajectories for time $t = 20$, and then use our estimation technique to recover the rate of absorption on the boundary using the simulated data. The estimates in Figure 4.6a were obtained with 20 simulations, while those in Figure 4.6b were obtained with 30 simulations. We observe from these figures that we have good estimates, and that the accuracy of our estimate increases as the number of simulations used increases. This suggests that more identical experimental procedures should be considered when estimating the rate of absorption on the boundary in order to increase the accuracy of the estimate. In addition, we notice that the accuracy of the estimates decreases as the initial position of the particles moves farther away from the boundary. This is due to the fact that when the particles start far away from the boundary, it takes more time for them to get to the boundary and they spread out more compared to when the start closer to the boundary. To get a better estimate when the particles starts far away from the boundary, we can either increase the final time for the simulation

or increase the number of particle in the simulation.

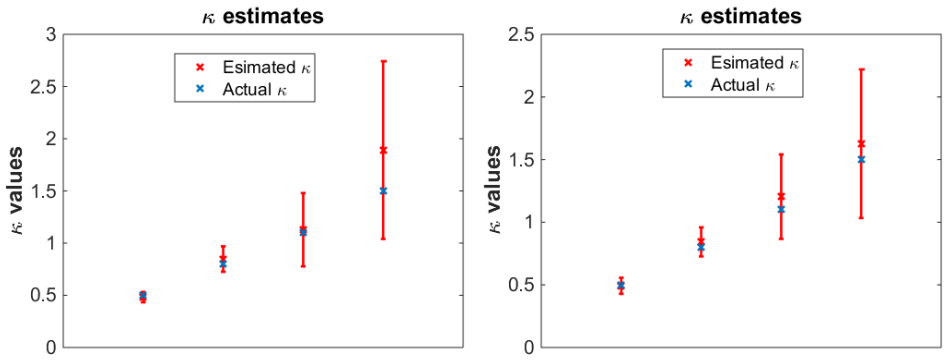

(a) **(b)**

Figure 4.7: Estimates of the rate of absorption on the boundary with standard deviation error bars based on simulated data using different κ values, for the half-plane problem.

In Figure 4.7, we show our estimates of the rate of absorption on the boundary with standard deviation error bars for a situation where we fixed the initial position of the particle and diffusion coefficient, but vary the rate of absorption on the boundary. The rates of absorption used are $0.5, 0.8, 1.1$, and 1.5, with diffusion coefficient $D = 0.1$, final time $t = 20$, and particle initial position $x_0 = 2$. The result in Figure 4.7a was obtained using 20 different simulations, while that of Figure 4.7b was obtained using 30 simulations. Similar to the estimates in Figure 4.6, we observe that the estimates get better as the number of simulations increases, although this comes at the expense of computational time.

Next, we present similar results for the disk problem. Figure 4.8 shows the estimates of the rate of absorption on the boundary of the disk-shaped region with standard deviation error bar. For these estimates, we consider a region of radius $a = 5$, with rate of absorption on the boundary $\kappa = 0.5$, diffusion coefficient $D = 0.1$, final time $t = 20$, and vary the initial position of the particles. We used 10 different simulations to obtain the estimates in Figure 4.8a and 20 simulations for those in Figure 4.8b. We notice from this figure that we also have better estimates when the particle starts close to the boundary and when we use more simulations

like in the case of the half-plane problem.

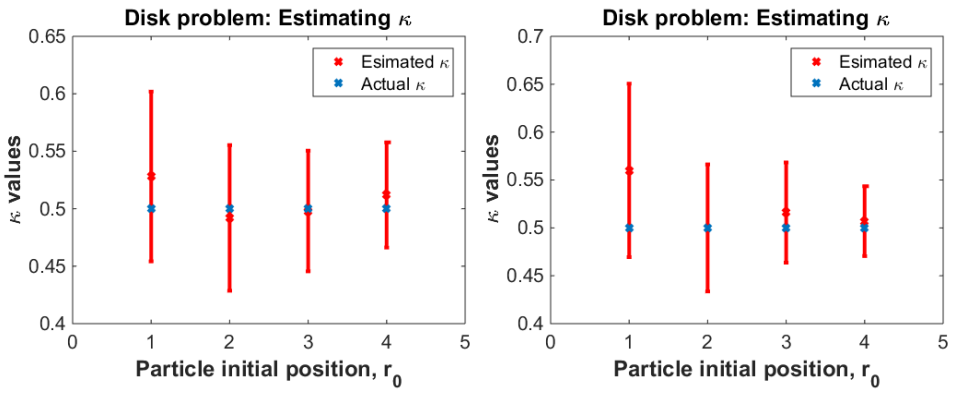

Figure 4.8: Estimates of the rate of absorption on the boundary with standard deviation error bars based on simulated data considering different particle initial positions r_0, for the disk problem.

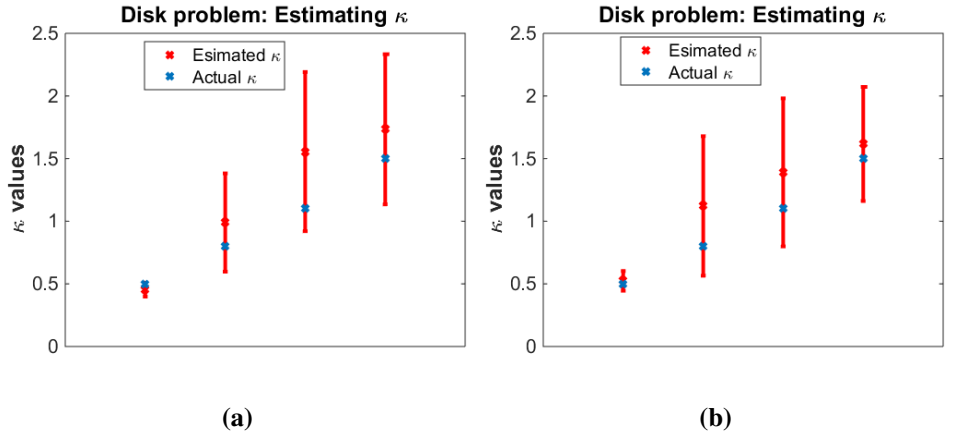

Figure 4.9: Estimates of the rate of absorption on the boundary with standard deviation error bars based on simulated data using different κ values, for the disk problem.

Figure 4.9a shows the estimates of the rate of absorption on the boundary of a disk-shaped region with standard deviation error bar for a case where we varied the rate of absorption on the boundary. We used the same value of the parameters

a, D, and t, as that of Figure 4.8, with initial position $r_0 = 2$, and vary the rate of absorption on the boundary. The κ values used for this figure are $0.5, 0.8, 1.1$, and 1.5. Similar to the right half-plane problem, we observe that the accuracy of our estimates decreases as the rate of absorption on the boundary increases.

In the next chapter, we shall consider a situation where the rate of absorption on the boundary fluctuates over time.

Chapter 5

Fluctuating Boundary

In this chapter, we consider scenarios where the boundary fluctuates from one boundary type to another. This chapter is motivated by a situation where the barrier causing the boundary is made up of some other diffusing particles. We present a technique for estimating the rate of absorption on the boundary by approximating the fluctuating boundary with a specific partially absorbing boundary. Furthermore, we consider a situation where the boundary switches between two boundary types at a specified time interval, and present mathematical relations for finding the effective rate of absorption on the boundary as a function of the switching time.

5.1 Estimating the rate of absorption on a fluctuating boundary

So far we have been discussing boundaries without taking a close look at the material that forms the boundaries. We know that in some cases, the barrier causing the boundary is not fixed. For example in cellular biology, molecules diffusing at a slow rate, and with high density may restrict the motion of some other molecules diffusing at a higher rate, thereby forming a boundary for these molecules. Figure 5.1a shows an illustration of a particle performing Brownian motion in the right half-plane (in black), where some other particles also performing Brownian motion (in blue) create a barrier forming a boundary at $x = 0$, and Figure 5.1b shows an illustration of a particle performing Brownian motion in a disk-shaped region

bounded by some particles that are also diffusing.

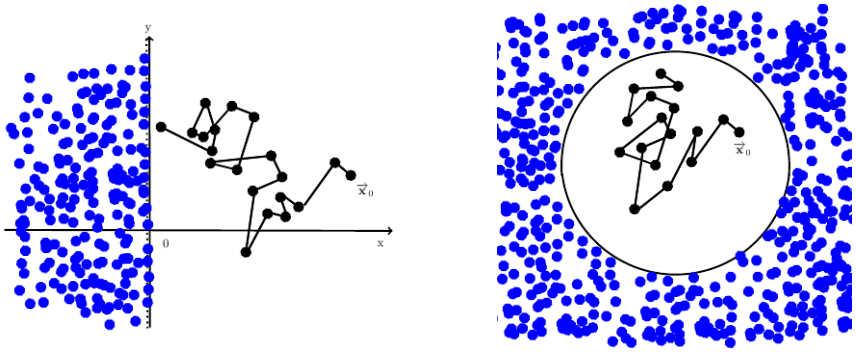

(a) The right half-plane.

(b) A disk-shaped region.

Figure 5.1: A particle performing Brownian motion in some region bounded by some other diffusing particles.

In this situation, we do not expect the boundary to be perfectly absorbing (or transmitting) or perfectly reflecting for all time, rather we would expect it to fluctuate between perfectly reflecting and partially absorbing over time. This boundary can also be seen as a stochastic switching boundary (see [8]) where the switching rate depends on the diffusion coefficient of the particles that create the barrier. An important question to ask is: *How can we estimate the rate of absorption on the boundary?*

Since the boundary fluctuates between partially absorbing and perfectly reflecting, we can model this boundary with a time varying Robin boundary condition, that is, we let the rate of absorption in the Robin boundary condition depends on time, as shown below,

$$D\frac{\partial P}{\partial x} = \kappa(t)P\,, \tag{5.1}$$

where $\kappa(t)$ is the time-dependent rate of absorption on the boundary.

Note that we are only considering a situation where the particle of interest (black in Figure 5.1) is either absorbed by the boundary or reflected back into the domain. Also, we assume that the boundary can never be free of the molecules that create the barrier, that is , the boundary is never perfectly absorbing.

The challenge with this problem is solving the PDE in Equation (4.1) together with the time varying Robin boundary condition analytically. As a result of this, we consider a much simpler Robin boundary condition using mean field approximation,

$$D\frac{\partial P}{\partial x} = \overline{\kappa}P, \tag{5.2}$$

where $\overline{\kappa}$ is the average of the rates of absorption on the boundary over time.

Now we can approximate the fluctuating boundary with a partially absorbing boundary where the rate of absorption on the boundary is the average of the fluctuating rates of absorption on the boundary.

For the half-plane problem, we have $\Omega = \{(x,y)\,|\,0 \le x < \infty,\ -\infty < y < \infty\}$. The probability that the particle of interest is at position $\overrightarrow{\mathbf{x}}$ at time t given that it started at $\overrightarrow{\mathbf{x}}_0$ at time $t = 0$, $P(\overrightarrow{\mathbf{x}}, t\,|\,\overrightarrow{\mathbf{x}}_0, 0)$ satisfies the following problem;

$$\begin{aligned}
&\frac{\partial P}{\partial t} = D\nabla^2 P, \quad \overrightarrow{\mathbf{x}} \in \Omega,\ t > 0,\\
&P(\overrightarrow{\mathbf{x}}, 0) = \delta(\overrightarrow{\mathbf{x}} - \overrightarrow{\mathbf{x}}_0),\\
&D\frac{\partial P}{\partial x} = \overline{\kappa}P, \quad \text{on } x = 0,\ -\infty < y < \infty,\\
&P \longrightarrow 0, \quad \text{as } x \longrightarrow \infty.
\end{aligned} \tag{5.3}$$

Notice that this problem is exactly the same with the problem in Equation (4.1) if we replace $\overline{\kappa}$ with κ. Therefore, we adopt the solution in Equation (4.11), and so we have that the probability distribution function for finding the particle in the right half-plane at time t given that it started at x_0 is

$$\begin{aligned}
\Gamma(t|x_0) = 1 - \Bigg[&\left(1 + \frac{x_0}{(x_0 + 2t\overline{\kappa})}\right)\frac{2t\,\overline{\kappa}}{(x_0 + 2t\overline{\kappa})}\,\operatorname{erfc}\left(\frac{x_0}{\sqrt{4Dt}}\right)\\
&- \frac{4(Dt)^{3/2}\overline{\kappa}}{\sqrt{\pi}D(x_0 + 2t\overline{\kappa})^2}\exp\left(-\frac{x_0^2}{4Dt}\right)\Bigg],
\end{aligned} \tag{5.4}$$

where $\overline{\kappa}$ is the average of the rates of absorption on the boundary over time.

Similarly, for a disk-shaped region, $\Omega = \{(r,\theta)\,|\,0 < r \le a, 0 \le \theta \le 2\pi\}$, and the probability of finding the particle of interest at position $\overrightarrow{\mathbf{x}} = (r,\theta)$ at time t

given that it started at position $\overrightarrow{\mathbf{x}}_0 = (r_0, \theta_0)$ at time $t = 0$ satisfies

$$\begin{aligned} &\frac{\partial P}{\partial t} = D\nabla^2 P, \ \overrightarrow{\mathbf{x}} = (r,\theta) \in \Omega, \ t > 0, \\ &\quad D\frac{\partial P}{\partial n} = -\overline{\kappa} P, \quad \text{on } \partial\Omega, \\ &\quad P \text{ is finite as } r \longrightarrow 0, \\ &\quad P(\overrightarrow{\mathbf{x}}, 0) = \delta(\overrightarrow{\mathbf{x}} - \overrightarrow{\mathbf{x}}_0). \end{aligned} \tag{5.5}$$

From Equation (4.36), the probability distribution function for finding the particle in the disk-shaped region at t given that it started at a distance r_0 from the center of the region is

$$\Gamma(t|r_0) = 2D^2 \sum_{m=1}^{\infty} \frac{\beta_m J_0\left(\frac{\beta_m}{a} r_0\right) J_1(\beta_m)}{\left(D^2\beta_m^2 + \overline{\kappa}^2 a^2\right) J_0^2(\beta_m)} \exp\left(-D\frac{\beta_m^2}{a^2} t\right). \tag{5.6}$$

where $\overline{\kappa}$ is the average of the rates of absorption on the boundary over time.

Next, we verify that the mean field approximation works for these problems by simulating trajectories in a region where the rate of absorption on the boundary fluctuates over time, and then calculate the probability of finding a particle performing Brownian motion inside the region from the simulation. In our simulation, we let the switching on the boundary happen at every unit time interval, and then calculate the average rate of absorption on the boundary which will be used in the probability distribution functions in Equations (5.4) and (5.6).

Figure 5.2 shows the fluctuation in the rate of absorption on the boundary over time, and the comparison of the probability for finding the particle of interest in the right half-plane calculated from simulation and the result obtained using mean field approximation, while Figure 5.3 shows similar results for a disk-shaped region of radius $a = 5$. For these figures, we averaged over 10 simulations, each with $10,000$ trajectories, with diffusion coefficient $D = 0.1$, $x_0 = 5$ for the half-plane problem, and $r_0 = 2$ for the disk problem. Although the rates of absorption on the boundaries of the two regions fluctuate over time in the simulations, the probability of finding the particle of interest in the regions obtained using the mean field approximation still agrees with the probability calculated form simulation. This

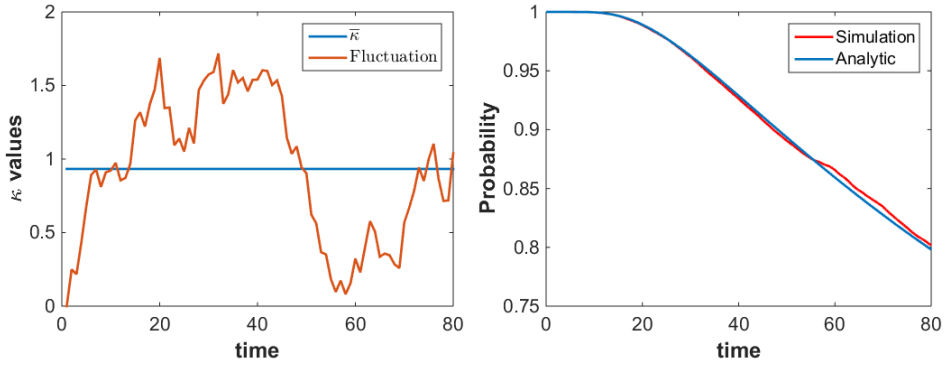

(a) Fluctuation on the boundary in terms of κ.

(b) Prob. of finding the particle in the right half-plane.

Figure 5.2: Comparison of the probability of finding the particle of interest in the right half-plane calculated from the simulation and the prediction from the mean field approximation.

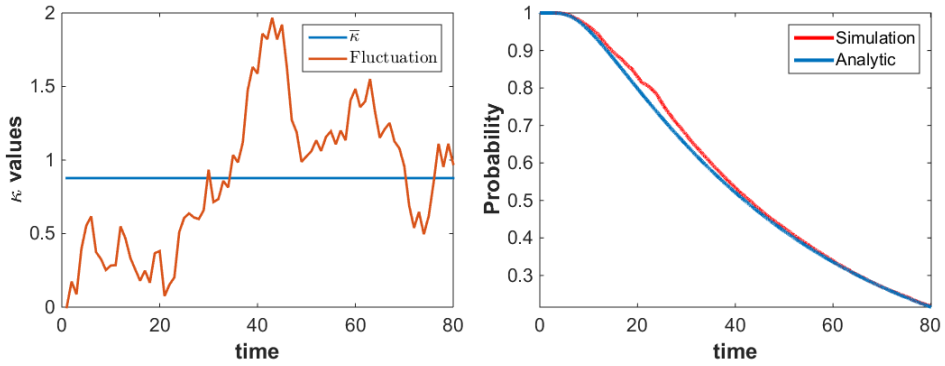

(a) Fluctuation on the boundary in terms of κ.

(b) Prob. of finding the particle in the disk-shaped region.

Figure 5.3: Comparison of the probability of finding the particle of interest in the a disk-shaped region calculated from the simulation and the prediction from the mean field approximation.

shows that the mean approximation works for these problems and that the effective rate of absorption on the boundary is the average of the fluctuating rates of absorption. It is also true that this mean field approximation works in a situation where the switching on the boundary happens at random.

5.2 Switching boundary

In this section, we consider situations where the boundary switches between two specific boundary types. First, we consider a case where the boundary switches between a perfectly reflecting boundary and a specific partially absorbing. Followed by the case where the boundary switches between a perfectly absorbing boundary and a perfectly reflecting boundary. For both cases, we approximate the switching boundary with a partially absorbing boundary, where the rate of absorption on the boundary is the effective rate of absorption that best approximates the solution, given the switching on the boundary. We also derive an empirical mathematical relation for the effective rate of absorption as a function of the boundary switching time.

5.2.1 Switching between perfectly reflecting and partially absorbing

Suppose the boundary of the region where the particle is performing Brownian motion switches between a perfectly reflecting boundary and a specific partially absorbing boundary at some specified time interval. Since a perfectly reflecting boundary condition can be obtained from the Robin boundary condition by setting the rate of absorption on the boundary to be zero (i.e $\kappa = 0$), we approach this problem from the point of view of a partially absorbing boundary with rate of absorption that switching between two specific rates (say, $\kappa_1 = 0$ and κ_2). We begin by setting the effective rate of absorption on the boundary to be the average of the two rates of absorption, that is, $\kappa_{eff} = \overline{\kappa}$. To validate this approximation, we simulate trajectories in a region where the rate of absorption on the boundary switches between these two rates, and from the simulation, we calculate the probability of finding the particle in the region at each time step and compare with the result of the appropriate probability distribution function.

Since we are approximating the switching boundary with a partially absorbing boundary whose rate of absorption is κ_{eff}, the resulting problem is the exactly the same as problem (4.1) for the half-plane problem and problem (4.18) for the disk problem with κ replaced by κ_{eff}. Therefore, the probability distribution function

for finding the particle in the right half-plane is,

$$\Gamma(t|x_0) = 1 - \left[\left(1 + \frac{x_0}{(x_0 + 2t\,\kappa_{eff})} \right) \frac{2t\,\kappa_{eff}}{(x_0 + 2t\,\kappa_{eff})} \operatorname{erfc}\left(\frac{x_0}{\sqrt{4Dt}} \right) - \frac{4(Dt)^{3/2}\kappa_{eff}}{\sqrt{\pi}D(x_0 + 2t\,\kappa_{eff})^2} \exp\left(-\frac{x_0^2}{4Dt} \right) \right]. \tag{5.7}$$

While that of a disk-shaped region is,

$$\Gamma(t|r_0) = 2D^2 \sum_{m=1}^{\infty} \frac{\beta_m J_0\left(\frac{\beta_m}{a} r_0\right) J_1(\beta_m)}{\left(D^2\beta_m^2 + \kappa_{eff}^2 a^2\right) J_0^2(\beta_m)} \exp\left(-D\frac{\beta_m^2}{a^2} t \right). \tag{5.8}$$

Figure 5.4 shows the comparison of the probabilities calculated from simulation and that of the probability distribution function in Equation (5.7).

We notice from these plots that irrespective of the value of κ_2, there is always a discrepancy between the result from the probability distribution function and that of the simulation. This suggests that the average of the rates of absorption on the boundary is not the effective rate of absorption. We have presented the plots for the right half-plane problem only. The analogous results for the disk problem have a similar discrepancy.

The next question is; *How can we find the effective rate of absorption on the boundary*? To answer this question, we fit the probability distribution function in Equation (5.7) to the probability of finding the particle in the right half-plane calculated from simulation as shown is Figure 5.5. The κ value that best fits the distribution function to the result from simulation is the effective rate of absorption on the boundary κ_{eff}. Following the same procedure, we can fit the probability distribution function in Equation (5.8) to simulated results to get the effective rate of absorption on the boundary for the case of a disk-shaped region.

Our goal is to derive a mathematical relation that predicts the effective rate of absorption κ_{eff} as a function of the rate of absorption κ_2 and the *switching time* of the boundary. We define the *switching time* as a regular time interval at which the boundary switches from one boundary type to the other, and denote it by α. Since we can get the effective rate of absorption on the boundary by fitting a probability distribution function to the probability for finding the particle in the region of

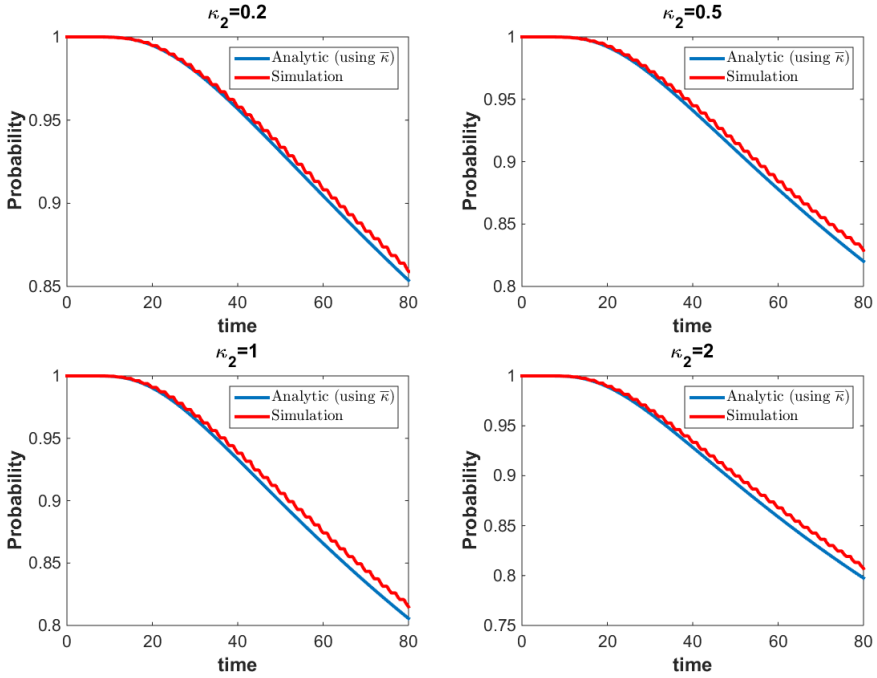

Figure 5.4: Comparison of the probability of finding the particle of interest in the right half-plane calculated from simulation and that of the probability distribution function in Equation (5.7).

interest calculated from simulation, we begin by doing this for different values of α. The values of α considered are between $1/2$ and 4 with an increment of $1/2$. Figure 5.6 shows the estimates of the effective rate of absorption obtained by fitting the probability distribution functions in Equations (5.7) and (5.8) to the probability calculated from simulation for different rate of absorption κ_2 and switching time. For the estimates in this figure, we averaged over 10 different simulations each with $10,000$ trajectories, diffusion coefficient $D = 0.1$, initial position $x_0 = 5$ for the right half-plane problem, and $r_0 = 2$ for the disk problem with a disk-shaped region of radius $a = 5$. We notice from this figure that the estimates for the half-plane problem is similar to that of the disk problem. Also, we observe that for each value of α, the effective rate of absorption converges to a particular value as κ_2 increases, and this asymptote value of κ_{eff} decreases as the switching time increases. These

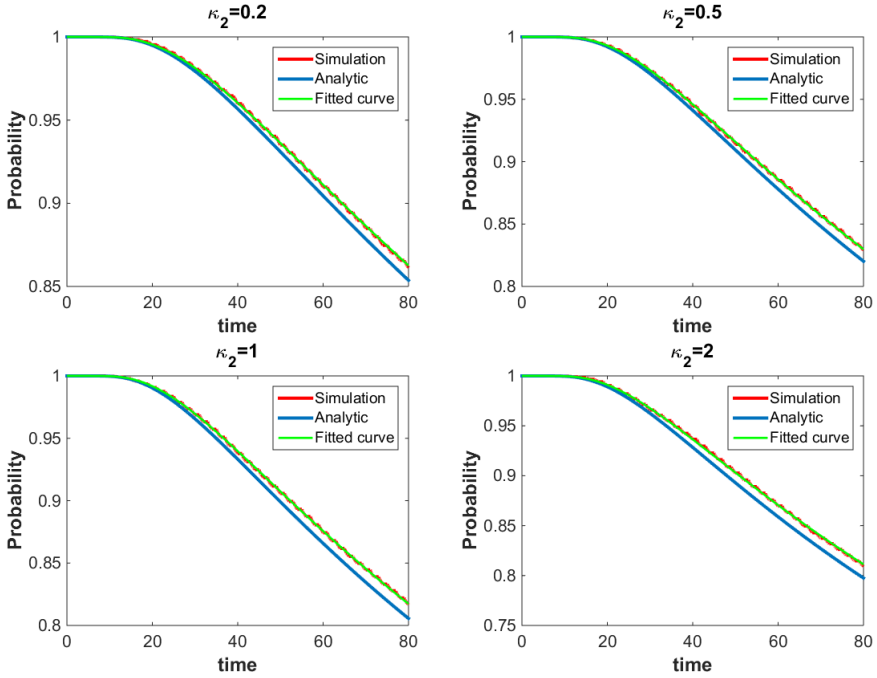

Figure 5.5: Fitting the probability distribution function in Equation (5.7) to result calculated from simulation in order to get the effective rate of absorption on the boundary.

plots suggest that the relationship between the effective rate of absorption, κ_2, and switching time can be approximated by the function

$$\kappa_{eff}(\alpha;\kappa_2) = f(\alpha)\left[1-\exp\left(-g(\alpha)\kappa_2\right)\right], \tag{5.9}$$

where $f(\alpha)$ and $g(\alpha)$ are *saturation* and *rate* functions, respectively, to be determined by fitting the model to the curves in Figure 5.6. We call $f(\alpha)$ a *saturation* function because it predicts where the values of κ_{eff} will saturate for each switching time, and $g(\alpha)$ a *rate* function because it gives the growth rate of κ_{eff} for each switching time.

Next, we fit the model in Equation (5.9) to each of the curves in Figure 5.6 to get the values of the functions $f(\alpha)$ and $g(\alpha)$ for each switching time α. The results of the fits are shown in Figure 5.7. We observe from these plots that the

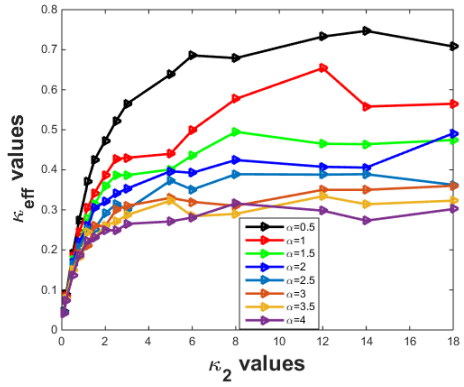

(a) Estimates for half-plane problem.

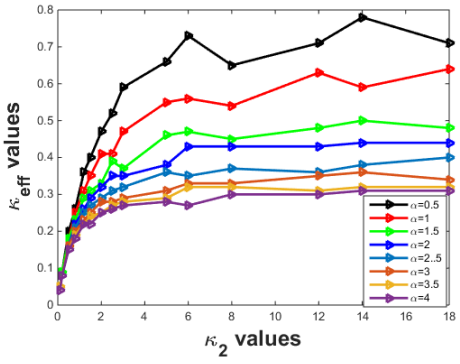

(b) Estimates for disk problem.

Figure 5.6: Estimates of the effective rate of absorption κ_{eff} obtained by fitting probability distribution functions to the simulated results for different values of κ_2 and switching time.

estimates for the functions $f(\alpha)$ and $g(\alpha)$ for the two geometries are very similar.

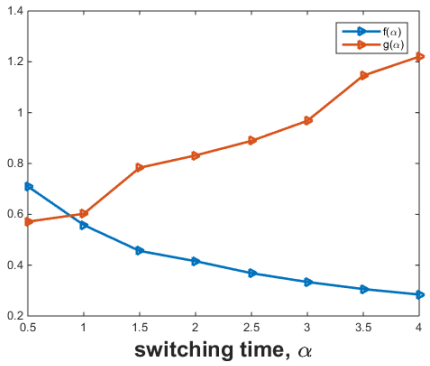

(a) Estimates for half-plane problem.

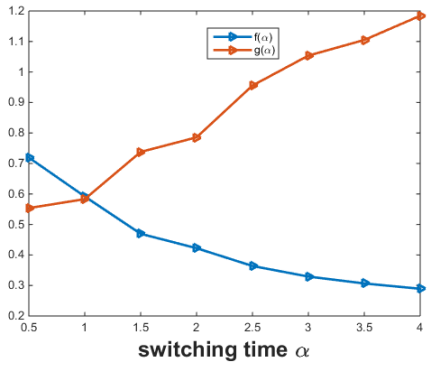

(b) Estimates for disk problem.

Figure 5.7: Estimates of the values of the functions $f(\alpha)$ and $g(\alpha)$ obtained by fitting the model in Equation (5.9) to the curves in Figure 5.6.

Lastly, we fit a linear polynomial to the curves of $g(\alpha)$ in Figure 5.7 using the

polyfit command in MATLAB, and for the saturation function, we fit the function

$$f(\alpha) = \frac{\mu_1}{1 + \left(\frac{\alpha}{\mu_2}\right)}, \tag{5.10}$$

to the curve of $f(\alpha)$ in Figure 5.7 using the least squares curve fitting tool in MATLAB. The parameters μ_1 and μ_2 are to be determined from the fit.

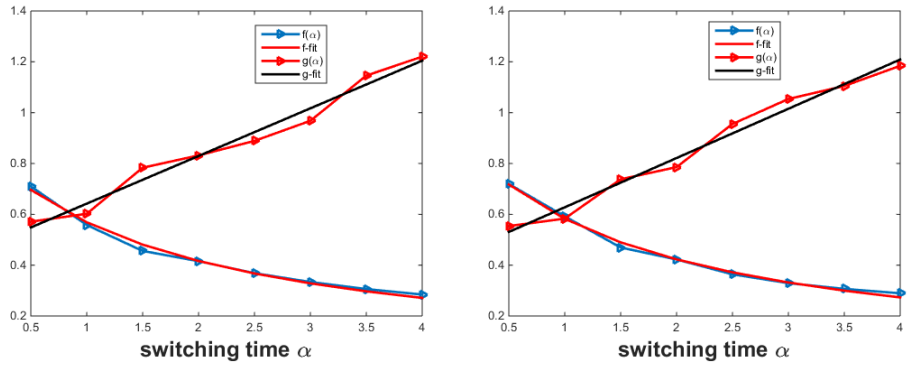

(a) Fits for half-plane problem.

(b) Fits for disk problem.

Figure 5.8: Fittings functions to the estimated values for the functions $f(\alpha)$ and $g(\alpha)$.

For the right half-plane problem, the functions obtained from the fittings are

$$f(\alpha) = \frac{0.8970}{1 + \left(\frac{\alpha}{1.7318}\right)}, \text{ and } g(\alpha) = 0.1875\alpha + 0.4545. \tag{5.11}$$

And for the disk problem, we obtain

$$f(\alpha) = \frac{0.9344}{1 + \left(\frac{\alpha}{1.6515}\right)}, \text{ and } g(\alpha) = 0.1938\alpha + 0.4337. \tag{5.12}$$

We notice that the functions $f(\alpha)$ and $g(\alpha)$ for the half-plane problem and the disk problem are very similar. These equations can be used together with the model in Equation (5.9) to predict the effective rate of absorption on the boundary as a function of the rate of absorption κ_2 and the switching time, for a situation where the boundary switches between a perfectly reflecting boundary and a specific partially

absorbing boundary.

5.2.2 Switching between perfectly reflecting and perfectly absorbing

In this section, we consider a situation where the boundary switches between perfectly absorbing and perfectly reflecting. Similar to the case of Section 5.2.1, we want to approximate the switching boundary with a partially absorbing boundary, where the rate of absorption on the boundary is the effective rate of absorption. Following a similar approach to that of Section 5.2.1, we derive a mathematical relation for the effective rate of absorption on the boundary as a function of the switching time. We consider the right half-plane problem and the disk problem, with different switching time. For each switching time, we simulate trajectories and calculate the probability of finding a particle performing Brownian motion in the region of interest. Then we fit the probabilities obtained from the simulation to the appropriate probability distribution function in order to estimate the effective rate of absorption on the boundary.

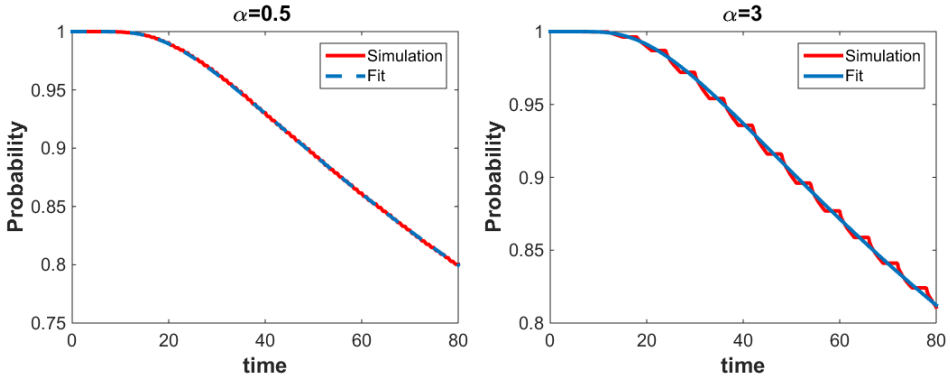

(a) Boundary switches every 0.5 time units. **(b)** Boundary switches every 3 time units.

Figure 5.9: Fitting the probability distribution function in Equation (5.7) to the probability calculated from simulation.

Figure 5.9 shows some of the fits of the probability distribution function in Equation (5.7) to simulated results, while Figure 5.10 shows the fits of the probability distribution function in Equation (5.8) to simulated result. For these plots, we averaged over 10 simulations each with $10,000$ particles, $D = 0.1$, $x_0 = 5$, $a = 5$,

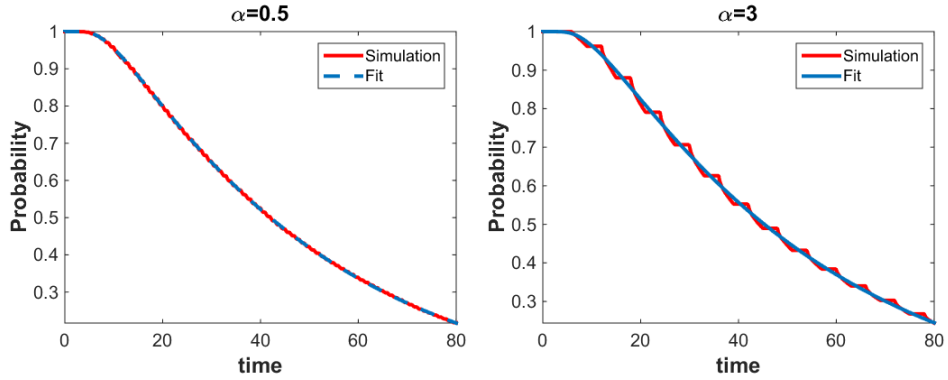

(a) Boundary switches every 0.5 time units. **(b)** Boundary switches every 3 time units.

Figure 5.10: Fitting the probability distribution function in Equation (5.8) to the probability calculated from simulation.

and $r_0 = 2$.

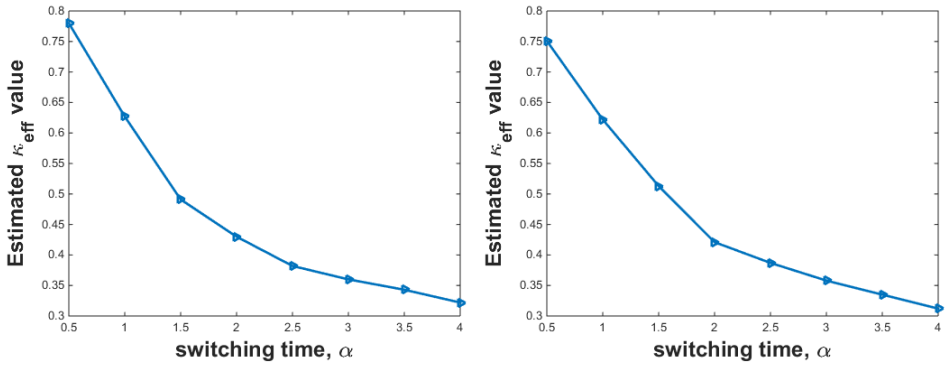

(a) Estimates for half-plane problem. **(b)** Estimates for disk problem.

Figure 5.11: Estimates of the effective rate of absorption κ_{eff} obtained by fitting probability distribution functions to the probability calculated from simulation.

For this case, we also considered switching time between $1/2$ and 4 with an increment of $1/2$, and for each value of α, we fit the distribution functions to the simulated probability to get effective rate of absorption κ_{eff}. The results of our estimates are shown is Figure 5.11. We notice from the curves in this figure that as

the switching time increases, the estimated values of the effective rate of absorption on the boundary decreases. These plots suggest modelling the relationship between the effective rate of absorption and the switching time with a decaying function.

Similar to the results in Section 5.2.1, the estimates of the effective rate of absorption for the half-plane problem and the disk problem are very similar. We also observe that these curves are similar to the curves for the saturation function $f(\alpha)$ in Figure 5.7. For this reason, we fit a function similar to the one in Equation (5.10) to these curves;

$$\kappa_{eff}(\alpha) = \frac{\gamma_1}{1+\left(\frac{\alpha}{\gamma_2}\right)}, \tag{5.13}$$

where γ_1, and γ_2 parameters to be determined from the fit.

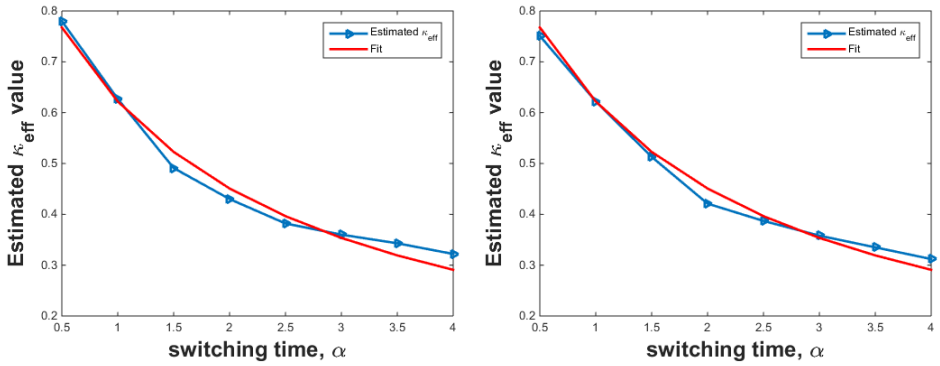

(a) Fits for half-plane problem. **(b)** Fits for disk problem.

Figure 5.12: Fitting the model in Equation (5.13) to the estimated effective rates of absorption in Figure 5.12.

Fitting the function in Equation (5.13) to the curves in Figure 5.12 using least squares curve fitting tool in MATLAB, we obtained the same values for the parameters γ_1 and γ_2 for the right half-plane problem and the disk problem. Therefore, the relation for the effective rate of absorption for the two geometry is the same and it is

$$\kappa_{eff}(\alpha) = \frac{1.0023}{1+\left(\frac{\alpha}{1.6349}\right)}. \tag{5.14}$$

Thus, we can approximate a boundary that switches between perfectly absorbing and perfecting reflecting with a partially absorbing whose rate of absorption is determined using this relation.

Chapter 6

Discussion and Conclusion

We have presented a mathematical technique for identifying a partially absorbing biological boundary, and also techniques for estimating the rate of absorption on such a boundary. These techniques are based on the probability of finding a particle performing Brownian motion in some region of a domain.

The first chapter of this thesis gives a brief introduction to biological boundaries, the kind of biological boundaries we are interested in, and some of the biological terms used in this project. We also presented a brief description of the single particle tracking experiment that motivated this project.

In the second chapter, we derived the diffusion equation from a simple one dimensional random walk process and used the derived equation to set-up our mathematical problem. Also in this chapter, we gave a brief introduction to a partially absorbing boundary and the Robin boundary condition, and presented some relations between the rate of absorption on the boundary in the Robin boundary condition and the probability of absorption on the boundary, derived by Erban and Chapman [4], and Steven Andrews [1].

The third chapter involves deriving probability distribution functions for finding a particle performing Brownian motion in some region of a two dimensional domain. We considered an unbounded domain, and a bounded domain in rectangular and polar coordinates. For the unbounded domain, we derived the probability distribution function for finding the particle in some region of the domain. To do this, we assumed that there is a region of the unbounded domain that is bounded

by an 'imaginary' boundary, and then derive the probability distribution function for finding the particle in this region at time t. This boundary is imaginary because it does not restrict the motion of the particle in and out of the region. For the bounded domain, we considered the right half-plane with an absorbing boundary at $x = 0$, and a disk-shaped region also with an absorbing boundary, and then derived the probability distribution function for finding the particle in these regions. Since these distribution functions give us the likelihood of finding the particle of interest in some region over time, we can fit these functions to experimental data to determine whether or not the experimental particle is experiencing a restricted motion. In order to do this, we need to consider the scenario that best models our experimental set-up and collect information such as the initial position of the particle, its diffusion coefficient, and the suspected locations of the boundary from the experiment. Substituting these pieces of information into the appropriate distribution function gives the distribution of probability for finding the particle in the designated region over time. Using this probability distribution together with the final position of the experimental particle, we can conclude whether or not the particle is experiencing a restricted motion and the possibility of a boundary.

Supposing we have identified a partially absorbing boundary, the next problem is to estimate the rate of absorption on the boundary. In the fourth chapter, we present a technique for estimating the rate of absorption on a partially absorbing boundary. This technique involves deriving a probability distribution function for finding a particle performing Brownian motion in a region bounded by a partially absorbing boundary. We considered two possible geometries: the right half-plane and a disk-shaped region. The probability distribution functions derived for each case contain a parameter that determines the rate of absorption on the boundary. These distribution functions are used together with maximum likelihood estimation to estimate that parameter based on simulated data. To do this, we first simulated trajectories using a specified rate of absorption on the boundary, and from this simulation, we collected the total number of particles that were absorbed on the boundary and those remaining in the region after a specified time. This information was substituted into the appropriate likelihood function derived using the relation in Equation (4.39), and then the resulting function was maximized with respect to κ to get the most probable rate of absorption on the boundary. Figures 4.6 - 4.9

show the results of our estimates of the rate of absorption on the boundary with standard deviation error bars for different parameter values. For Figures 4.6 and 4.8, we varied the initial position of the particle. We observe from these figures that we were able to recover the rate of absorption on the boundary with high level of accuracy for the cases where the particles start close the boundary, and as the initial position of the particle moves farther away from the boundary, our estimates become less accurate and the standard deviation increases. This is due to the fact that when the particles start far away from the boundary, they spread out more, therefore, it takes them longer to get to the boundary compared to when they start closer to the boundary. In Figures 4.7 and 4.9, we fixed the initial position of the particle and varied the rate of absorption on the boundary. We can see from these figures that we have good estimates when the rate of absorption on the boundary is small, and as κ increase, the accuracy of our estimates decreases and the variance also increases.

We also looked at a scenario where the boundary of the region in which the particle is performing Brownian motion is formed by some other diffusing particles, and as a result of the motion of the particles forming the barrier, the boundary fluctuates between a perfectly reflecting boundary and partially absorbing boundaries. To estimate the rate of absorption on the boundary, we used mean field approximation to approximate the fluctuating boundary with a partially absorbing boundary where the rate of absorption on the boundary is the average of the fluctuating rates of absorption. To verify that this approximation works, we simulate trajectories in a region bounded by a fluctuating boundary, and calculate the probability that the particle performing Brownian motion is still inside the region at time t from the simulation. In the simulation, the boundary switches from one boundary type to another at every unit time interval, and the probability calculated from it is compared to the result obtained from the probability distribution function derived using the mean field approximation (that is, Equation (5.4) for the half-plane problem and Equation (5.6) for the disk problem). The comparison of the two probabilities is shown in Figure 5.2 for the right half-plane problem and in Figure 5.3 for the disk problem. We notice from these figures that the two result agree to a large extent, this shows that the mean field approximation works for this scenario. Thus, we conclude that the fluctuating boundary in this scenario can be approximated by

a partially absorbing boundary whose rate of absorption on the boundary is the average of the fluctuating rates of absorption.

Furthermore, we considered a scenario where the boundary switches between two boundary types at specified time interval. The first case considered is when the boundary switches between a perfectly reflecting boundary and a specific partially absorbing boundary (with rate of absorption on the boundary labelled as κ_2), while the other case is when it switches between a perfectly reflecting and a perfectly absorbing boundary. We approximate these switching boundaries with a partially absorbing boundary, where the rate of absorption on the boundary is the rate of absorption that best approximates the solution, given the switching on the boundary, and it is called the effective rate of absorption denoted by κ_{eff}. For each of the two cases, we derived a mathematical relation for finding the effective rate of absorption on the boundary a function of the switching time. To get the relation for the first case, we simulate trajectories in a region where the boundary switches between the two boundary types. From the simulation, we calculate the probability that a particle performing Brownian motion in this region is still in the region at time t, and then fit the appropriate probability distribution function to the calculated probability in order to get the rate of absorption on the boundary that best fits the simulated result. This rate of absorption is the effective rate of absorption on the boundary. Figure 5.6 shows the fits for several values of κ_2 and different switching time, for the half-plane problem and the disk problem. Next, we fit the model in Equation (5.9) to the estimates in Figure 5.6 in order to get the values for the saturation function $f(\alpha)$, and the rate function $g(\alpha)$ for each switching time α. And lastly, we fit functions to the curves of $f(\alpha)$ and $g(\alpha)$ obtained from the previous fits. The mathematical relation obtained for the effective rate of absorption κ_{eff} for the right half-plane problem is given as

$$\kappa_{eff}(\alpha;\kappa_2) = \left(\frac{0.8970}{1+\left(\frac{\alpha}{1.7318}\right)}\right)\left[1-\exp\left(-(0.1875\alpha+0.4545)\kappa_2\right)\right]. \qquad (6.1)$$

And that of the disk problem is

$$\kappa_{eff}(\alpha;\kappa_2) = \left(\frac{0.9344}{1+\left(\frac{\alpha}{1.6515}\right)}\right)\left[1-\exp\left(-(0.1938\alpha+0.4337)\kappa_2\right)\right], \qquad (6.2)$$

where α is the switching time, and κ_2 is the rate of absorption for the partially absorbing boundary that switches.

We notice that the relations for the effective rate of absorption on the partially absorbing boundary for the two geometries are very similar. This suggests that the rate for this scenario is independent of the geometry of the region, rather it dependent on κ_2 and switching time. We believe that the slight difference in the results is as a result of approximation errors and the stochastic nature of our approach. Thus, in a situation where a boundary switches between a perfectly reflecting boundary and a specific partially absorbing boundary, this boundary can be replaced with a partially absorbing boundary where the rate of absorption on the boundary is obtained using the relations in Equations (6.1) and (6.2) appropriately.

For the case where the boundary switches between a perfectly reflecting boundary and a perfectly absorbing boundary, we used a similar approach of fitting probability distribution functions to the probabilities calculated from simulation in order to estimate the effective rate of absorption on the boundary. We then fit a function to these estimates to get a relation that predicts the effective rate of absorption on the boundary as a function of the switching time. The relation obtained for the right half-plane problem and the disk problem are exactly the same for this scenario, and it is given in Equation (5.14). This is in agreement with the suggestion in the previous scenario of switching boundary that the effective rate of absorption on the boundary is independent of the geometry. Therefore, we conclude that a boundary that switches between a perfectly reflecting and a perfectly absorbing boundary at regular time intervals can be approximated with a partially absorbing boundary whose rate of absorption in obtained using the relation in Equation (5.14).

We believe that the techniques presented in this project will help in identifying partially permeable biological boundaries, and also in estimating the rate of absorption on the boundaries. This will go a long way in enhancing our understanding the motion of biological particles, and the analysis of experimental data.

6.1 Future work

Future work in this direction would be to apply the techniques presented in this thesis to experimental data.

For the regions we have considered in this thesis, we have assumed that the boundaries are smooth, while in reality, biological boundaries may not be smooth. It would be interesting to develop a technique for estimating the rate of absorption on a rough boundary.

In addition, it would also be interesting to develop a technique for estimating the rate of transmission on a partially transmitting boundary. For a transmitting boundary, a diffusing particle can cross the boundary from both sides of the boundary. As a result of this, the boundary has two faces, each with a rate of transmission, and these rates are not necessarily the same. Developing a technique to estimates these rates of transmission would also be an interesting question.

Bibliography

[1] S. S. Andrews. Accurate particle-based simulation of adsorption, desorption and partial transmission. *Physical Biology*, 6(4):046015, 2009. URL http://stacks.iop.org/1478-3975/6/i=4/a=046015. → pages 11, 12, 72

[2] S. S. Andrews and D. Bray. Stochastic simulation of chemical reactions with spatial resolution and single molecule detail. *Physical Biology*, 1(3):137, 2004. URL http://stacks.iop.org/1478-3975/1/i=3/a=001. → pages 40, 52

[3] S. Chandrasekhar. Stochastic problems in physics and astronomy. *Reviews of Modern Physics*, 15, 1943. → pages 5

[4] R. Erban and S. J. Chapman. Reactive boundary conditions for stochastic simulations of reaction–diffusion processes. *Physical Biology*, 4(1):16, 2007. URL http://stacks.iop.org/1478-3975/4/i=1/a=003. → pages 11, 32, 72

[5] F. C. Goodrich. Random walk with semiadsorbing barrier. *Journal of Chemical Physics*, 22:588–594, 1954. → pages 5

[6] G. Lamm. Extended Brownian dynamics. iii. three-dimensional diffusion. *The Journal of chemical physics*, 80(6):2845–2855, 1984. → pages 5

[7] G. Lamm and K. Schulten. Extended Brownian dynamics. ii. reactive, nonlinear diffusion. *The Journal of Chemical Physics*, 78(5):2713–2734, 1983. → pages 5

[8] S. D. Lawley, J. C. Mattingly, and M. C. Reed. Stochastic switching in infinite dimensions with applications to random parabolic PDE. *SIAM Journal on Mathematical Analysis*, 47(4):3035–3063, 2015. → pages 58

[9] N. Ruthardt, D. C. Lamb, and C. Bräuchle. Single-particle tracking as a quantitative microscopy-based approach to unravel cell entry mechanisms of

viruses and pharmaceutical nanoparticles. *Molecular therapy*, 19(7): 1199–1211, 2011. → pages 2

[10] A. Singer, Z. Schuss, A. Osipov, and D. Holcman. Partially reflected diffusion. *SIAM Journal on Applied Mathematics*, 68(3):844–868, 2008. doi:10.1137/060663258. URL http://dx.doi.org/10.1137/060663258. → pages 5

[11] J. St-Pierre and H. L. Ostergaard. A role for the protein tyrosine phosphatase CD45 in macrophage adhesion through the regulation of paxillin degradation. *PloS one*, 8(7):e71531, 2013. → pages 3

[12] Wikipedia. Single particle tracking — wikipedia, the free encyclopedia, 2015. URL https://en.wikipedia.org/w/index.php?title=Single_particle_tracking&oldid=668616350. [Online; accessed 9-May-2016]. → pages 2

[13] Wikipedia. PTPRC — wikipedia, the free encyclopedia, 2016. URL https://en.wikipedia.org/w/index.php?title=PTPRC&oldid=733512364. [Online; accessed 29-April-2016]. → pages 3

[14] Wikipedia. Immunoglobulin g — wikipedia, the free encyclopedia, 2016. URL https://en.wikipedia.org/w/index.php?title=Immunoglobulin_G&oldid=731665299. [Online; accessed 29-April-2016]. → pages 3

[15] Wikipedia. Likelihood function — wikipedia, the free encyclopedia, 2016. URL https://en.wikipedia.org/w/index.php?title=Likelihood_function&oldid=726085070. [Online; accessed 2-May-2016]. → pages 12

[16] Wikipedia. Macrophage — wikipedia, the free encyclopedia, 2016. URL https://en.wikipedia.org/w/index.php?title=Macrophage&oldid=728586918. [Online; accessed 11-August-2016]. → pages 2

[17] Wikipedia. Marcum q-function — wikipedia, the free encyclopedia, 2016. URL https://en.wikipedia.org/w/index.php?title=Marcum_Q-function&oldid=717292997. [Online; accessed 3-May-2016]. → pages 19

[18] Wikipedia. Random walk — wikipedia, the free encyclopedia, 2016. URL https://en.wikipedia.org/w/index.php?title=Random_walk&oldid=718681846. [Online; accessed 30-May-2016]. → pages 8

[19] E. Zauderer. *Partial Differential Equations of Applied Mathematics*. John Wiley & Sons, Inc, CHoboken, New Jersey, Third Edition, 2016. → pages 35

Appendix A

Supporting Materials

Below are some of the smoldyn codes used to produce the results in this thesis. These scripts were called from MATLAB using some other scripts through which the value of the parameters such as simulation stopping time, simulation time step, initial number of particles, the staring position of the particles, and the different rates of absorptions on the boundary were supplied. In addition, the data obtained from these simulations are exported to Matlab for further processing.

A.1 Smoldyn code for partially absorbing boundary problem

```
# likelihood simulation
# rectangular Geometry

graphics opengl
#graphic_iter 5

dim 2     # specifying the dimension of the system
species A   # specifying particle species types
difc all 0.1   # specifying diffusion coefficient of particle
color A 1 0 0   # specifying the species color
display_size all 2.01 # specifying the display size particles
```

```
time_start 0 # specifying starting time of simulation
time_stop T_time # specifying stopping time of simulation
time_step T_step # specifying simulation time step

### defining system boundary
boundaries 0 0 100 r
boundaries 1 0 100 r
frame_thickness 0

### designing the simulation graphics interface
start_surface Right_rectangle
action front A reflect
color back black 0.2
color front blue 0.1
panel rect +0 0 0 100
panel rect -0 100 0 100
panel rect +1 0 100 100
panel rect -1 0 0 100
end_surface

### defining the partially absorbing boundary
start_surface Boundary
rate A bsoln fsoln Kappa # specifying the rate of absorption
                         # on the boundary
action A front reflect
color back red 0.2
panel rect -0 0 0 100
thickness 1
end_surface

### defining simulation region of interest
start_compartment right_compt
```

```
surface Right_rectangle
point 50 50
end_compartment

### specifying the initial number of particle (called 'total')
### and the start position
mol total A start_point 50

### defining the output file
output_files FILEROOT_out.txt stdout

### writing the total number of molecules left in the region
### into the output file at each simulation time step
cmd N 1 molcountincmpts right_compt FILEROOT_out.txt
cmd a molcount stdout

end_file
```

A.2 Smoldyn code for fluctuating boundary problem

```
# Fluctuating boundary simulation
# rectangular Geometry

graphics opengl
#graphic_iter 5

dim 2     # specifying the dimension of the system
species A   # specifying particle species types
difc all 0.1   # specifying diffusion coefficient of particle
color A 1 0 0   # specifying the species color
display_size all 2.01 # specifying the display size particles

time_start 0 # specifying starting time of simulation
```

```
time_stop T_time # specifying stopping time of simulation
time_step T_step # specifying simulation time step

### defining system boundary
boundaries 0 0 100 r
boundaries 1 0 100 r
frame_thickness 0

### designing the simulation graphics interface
start_surface Right_rectangle
action front A reflect
color back black 0.2
color front blue 0.1
panel rect +0 0 0 100 r1
panel rect -0 100 0 100 r2
panel rect +1 0 100 100 r3
panel rect -1 0 0 100 r4
end_surface

### defining the boundary that fluctuates
start_surface Boundary
action A front reflect
color back red 0.2
panel rect -0 0 0 100 rec1
thickness 1
end_surface

## specifying an initial rate of absoprtion on the boundary
surface Boundary rate A bsoln fsoln 0

### defining simulation region of interest
start_compartment right_compt
surface Right_rectangle
```

```
point 50 50
end_compartment

### specifying the initial number of particle (called 'total')
### and the start position
mol total A start_point 50

### defining the output file
output_files FILEROOT_out.txt stdout

### performing the switching on the boundary
cmd @ 1 set surface Boundary rate A bsoln fsoln aa
cmd @ 2 set surface Boundary rate A bsoln fsoln bb
cmd @ 3 set surface Boundary rate A bsoln fsoln cc
cmd @ 4 set surface Boundary rate A bsoln fsoln dd
cmd @ 5 set surface Boundary rate A bsoln fsoln ee
 : : : : :   : : :  : : : : :   : : : : :   : : :
 . . . . .   . . .  . . . . .   . . . . .   . . .
cmd @ 76 set surface Boundary rate A bsoln fsoln a75
cmd @ 77 set surface Boundary rate A bsoln fsoln a76
cmd @ 78 set surface Boundary rate A bsoln fsoln a77
cmd @ 79 set surface Boundary rate A bsoln fsoln a78
cmd @ 80 set surface Boundary rate A bsoln fsoln a79

### writing the total number of molecules left in the region
### into the output file at each simulation time step
cmd N 1 molcountincmpts right_compt FILEROOT_out.txt

end_file
```